V

MOLECULAR DYNAMICS: INTENSE EXTERNAL FIELDS

M. W. EVANS

CONTENTS

I. HISTORICAL DEVELOPMENT

The first worker to consider the detailed effect of a strong external force field on the molecular dynamics of an isotropic molecular liquid seems to have been Benoit.[1] This treatment may be developed considerably and extended.[2-4] In this review, however, the technique of computer simulation is used in combination with "reduced" model theory (see Chapter I) in an attempt to probe more deeply into the fundamental physical characteristics of the molecular liquid state.

This chapter is dedicated to the South Wales Branch of the National Union of Mineworkers.

By employing a very strong external field, a gedankexperiment may be set up whereby the natural thermal motion of the molecules is put in competition with the aligning effect of the field. This method reveals some properties of the molecular liquid state which are otherwise hidden. In order to explain the observable effects of the applied fields, it is necessary to use equations of motion more generally valid than those of Benoit. These equations may be incorporated within the general structure of "reduced" model theory[5-7] (RMT) and illustrate the use of RMT in the context of liquid-state molecular dynamics. (Elsewhere in this volume RMT is applied to problems in other fields of physics where consideration of stochastic processes is necessary.) In this chapter modifications to the standard methods[8] are described which enable the detailed study of field-on molecular dynamics.

In general there is no limit to the types of fields that can be considered in the gedankexperiment, or to the field strength, or to the permutations and combinations. As the field strength is increased, orientational characteristics at field-on equilibrium must be describable through Langevin functions of various kinds, and the molecular dynamics by the use of RMT. One of the first breakthroughs in this context came in the mid-1970s with the development by Grigolini[9-12] of a theory to describe the competition between preparation and relaxation in the field of radiationless decay. The case of excitation with strong fields was also considered. The field has a direct effect on a variable of interest, such as the molecular angular velocity $\boldsymbol{\omega}$, and isolates (or decouples) the characteristics of this variable from others in the molecular ensemble, or thermal bath. This decoupling effect was predicted[9] theoretically by Grigolini in 1976 in the context of spin relaxation[13] and radiationless decay in molecules.[9] Numerical evidence for Grigolini's predictions was provided by Evans,[14-18] using molecular dynamics computer simulation, and by Bagchi and Oxtoby,[19-20] using computer simulation of stochastic forces in a different context.

Recently, another fundamental property of the liquid state has been discovered by comparing the orientational fall transient from field-on to field-off equilibrium with the relevant orientational autocorrelation function.[21,22] According to classical (linear) fluctuation-dissipation theory, the fall-transient and autocorrelation function (acf) are identical. Computer simulations show that the fall transient decays to equilibrium more quickly, and sometimes much more quickly, than the acf when the field initially applied to the molecular liquid becomes greater than the thermal kT in energetic terms. This speeding up of the fall transient is referred to in this review as the *deexcitation effect*. The RMT is capable of exploring the numerical results analytically using new concepts of nonlinearity in the molecular liquid state. One of the results of this gedankexperiment may be described in simple terms

as follows. A Langevin equation of the type

$$\dot{\boldsymbol{\omega}}(t) = -\gamma\boldsymbol{\omega} + \mathbf{f}(t) \tag{1}$$

is a description of the field-off molecular dynamics which always implies that the normalized fall transient and the relevant field-off acf must be identical experimental decay functions of time. In the simple equation (1.1), $\boldsymbol{\omega}$ is the molecular angular velocity, γ a normalized friction coefficient, and $\mathbf{f}(t)$ a stochastic angular acceleration term. The new developments of nonlinear physics exemplified by and incorporated in RMT lead in certain long-time limits[22] to a fundamentally nonlinear structure such as

$$\dot{\boldsymbol{\omega}}(t) = -\gamma\boldsymbol{\omega}(t) + \gamma'\boldsymbol{\omega}(t)\langle\omega^2(t)\rangle + \mathbf{f}(t) \tag{2}$$

Note that, as discussed at length in Chapter VI, this equation has to be limited to providing information on $\langle\boldsymbol{\omega}(t)\rangle$. The influence of the nonlinear term on the time evolution of $\langle\omega^2(t)\rangle$ is not compatible with the attainment of a canonical equilibrium. This type of equation lends itself to a qualitative description of deexcitation effects as observed by computer simulation. This is described further in Section IV.A with reference to the general analytical constraints imposed by RMT on *any theory* of the molecular liquid state.

This review is developed as follows. In Section II the fundamental idea of field-on computer simulation is described with reference to the molecular dynamics of an achiral molecule of C_{2v} symmetry. The field-on computer-simulated orientational characteristics are tested with the equilibrium theory of statistical mechanics as embodied in Langevin and Kielich functions[18] of applied field strength. The characteristics of the molecular dynamics at field-on equilibrium are quantified in terms of auto- and cross-correlation functions. Of particular interest in this context is the autocorrelation function of the molecular angular velocity $\boldsymbol{\omega}$. This acf develops oscillations under the influence of the field which decay *slowly* as a function of time. *The envelope of these oscillations is longer lived than the acf at field-off equilibrium and is also dependent on the field strength.*[17] These are essentially the characteristics of the Grigolini decoupling effect.[9] The theorems embodied in RMT allow Grigolini and his coworkers to describe these effects analytically[21] and, in principle, quantitatively. Theories such as those of van Kampen and Praestgaard,[23] which are purely phenomenological in nature and fall outside the RMT framework, do not describe the decoupling effect and should therefore be modified a little according to the numerical results. The deexcitation effect is introduced[14] with reference to achiral triatomics of C_{2v} symmetry. The three-dimensional molecular dynamics in this case is a formidable challenge to three-dimensional analytical theory because of the im-

portant role played by rotation-translation coupling.[24] The RMT can, however, follow the guidelines laid down by the numerical method qualitatively, by restricting the analytical treatment to two dimensions as described in Section III. In this limit a version of Eq. (2) is successful[22] in describing the numerical deexcitation effect at least qualitatively. This equation is a limiting form of the nonlinear two-dimensional itinerant oscillator,[25] an RMT-allowed mathematical model of the liquid state.

In Section IV the computer simulation is extended to describe the effects of excitation in chiral molecules and racemic mixtures of enantiomers. The modification of the dynamical properties brought about by mixing two enantiomers in equimolar proportion may be explained in terms of rotation-translation coupling.[24] The application of an external field in this context amplifies the difference between the field-on acf's and cross-correlation of enantiomer and racemic mixture and provides a method of studying experimentally the fundamental phenomenon of rotation-translation coupling in the molecular liquid state of matter.

The mathematical and computational techniques developed in this review may hopefully be transferred in the future to deal with the problems of technical and industrial importance that depend for their description on nonlinear stochastic differential equations. Of particular importance in this context is the nonlinear technique needed for the description of hysteresis in the Josephson tunneling junction.[26] The circuitry of the newer generation of computers and integrated circuits in general is reaching the atomic level in dimensionality. In this limit the field strengths involved in calculating the boundary characteristics of the circuitry are very large. Stochastic equations are necessary for a complete description of the phenomena involved. The methods used in this review may also be used to describe the diffusion of charge carriers in semiconductors, chemical reaction rates, superionic conductors, dipole-dipole interaction in dielectric relaxation, cycle slips in second-order phase-locked loops, and other phenomena which involve the interaction of fields and stochastic variables. Several of these topics are described in detail using RMT elsewhere in this volume. A generalization of the available methods of solution will have a variety of other applications to problems of practical importance in a range of disciplines. Add to this the power of computer simulation, and it is possible to begin to construct a sound and general theoretical basis for a number of useful phenomena.

To conclude this introductory section, the *simplest* type of equation that should be considered for a useful description is a stochastic differential equation such as

$$\frac{d^2x(t)}{dt^2} + \zeta\frac{dx(t)}{dt} + \frac{dV(x)}{dx} = \lambda(t) \tag{3}$$

This is an equation written, for example, for a Brownian particle of mass m moving along the x axis under the influence of a potential $V(x)$. Here $\lambda(t)$ is a white-noise driving force (a stochastic variable) coming from the Brownian movement of the surroundings, and $\zeta\dot{x}(t)$ is the systematic friction force. This equation can be solved exactly only in the known special cases $V = 0$ and $V = \gamma x^2$, where γ is a coefficient independent of time. Equation (3) is the Langevin equation equivalent to the Kramers equation[5,6]

$$\frac{\partial G}{\partial t} + \dot{x}\frac{\partial G}{\partial x} - \frac{1}{m}\frac{\partial V}{\partial x}\frac{\partial G}{\partial \dot{x}} = \frac{\zeta}{m}\frac{\partial}{\partial \dot{x}}\left(\dot{x}G + \frac{kT}{m}\frac{\partial G}{\partial \dot{x}}\right) \tag{4}$$

for the complete phase-space conditional probability density function $G(x, \dot{x}, t|x(0), \dot{x}(0), 0)$ under the boundary condition $G(x, \dot{x}, 0) = \delta(x - x_0)\delta(\dot{x} - \dot{x}_0)$. *The same equations*, written for two-dimensional rotational Brownian motion in N-potential wells of the cosine type have been used by Reid[26] as a good description of the absorption spectra of dipolar molecular liquids in the frequency range from static terahertz (far infrared).[5]

These equations *cannot*, however, describe the deexcitation effect without some development within the general RMT structure. The RMT therefore provides a more generally valid description of liquid-state molecular dynamics than Eqs. (3) or (4). It is probable that the same is true for Josephson junction hysteresis in the presence of fields and related phenomena such as those described in the other reviews of this special volume.

The powerful continued fraction procedure (CFP) described by Grosso and Pastori Parravicini in Chapter III may be used to solve Eqs. (3) and (4). An alternative approach has been provided by Ferrario et al.,[25] who have computed a variety of numerically derived orientation and velocity acf's for a simple cosine potential and the more complicated cosinal itinerant oscillator, another RMT-allowed structure. In Chapter VI, Ferrario et al. describe deexcitation effects from the two-dimensional disk-annulus itinerant oscillator also studied by Brot and coworkers.[27]

Coffey, Rybarsch, and Schroer[3] have considered the numerical solution of the Kramers equations for two-dimensional rotation, which is the exact rotational counterpart of Eq. (3) or Eq. (4). These equations are also soluble numerically by use of the CFP for any value of field strength embodied in the potential V. When the field is very intense—for example, in boundaries of integrated circuits—the rise transient after switching on the field becomes oscillatory, as demonstrated analytically by Coffey et al.[3] and numerically by Evans (see Section IV). At field-on equilibrium, the Grigolini decoupling effect appears from a slightly more complicated RMT structure[21] than the level embodied in Eq. (3) or (4). As we have mentioned, a greater degree of sophistication is also required for an analytical description of the deexcitation effect (Section III).

The properties of equations such as (3) and (4) which are not allowed by RMT are understood satisfactorily only in the relatively uninteresting linear case where, for example, rise and fall transients mirror each other as exponentials.[1] When this frontier is crossed, the applied field strength is such that it is able to compete effectively with the intermolecular forces in liquids. This competition provides us with information about the nature of a molecular liquid which is otherwise unobtainable experimentally. This is probably also the case for *internal* fields, such as described by Onsager for liquids,[28,29] for various kinds of internal fields in integrated computer circuits, activated polymers,[30] one-dimensional conductors, amorphous solids, and materials of interest to information technology. The chapters by Grosso and Pastori Parravicini in this volume describe with the CFP some important phenomena of the solid state of matter in a slightly different context.

II. COMPUTER SIMULATION

Computer simulation of the effect of intense externally applied force fields on molecular liquids has been initiated recently by Evans in a series of articles.[14-18] The purpose of the computer simulation is to produce a self-consistent numerical data for discussion by analytical theoreticians and experimentalists in this area. Without the nonlinear potential term V the equations of Section I produce results which are wholly at odds with, for example, spectral data in the far infrared.[5] This is understood now to be due to the neglect of inertial effects and to the assumption that the friction coefficient does not evolve with time, that is, there are no memory effects. In the language of RMT, the infinite Mori continued fraction has been truncated at the first approximant, using Langevin's original dramatic separation of time scales or ("adiabatic elimination"), into a viscous drag coefficient varying infinitely slowly with time and a white-noise term [i.e., one whose autocorrelation function is a delta function decaying infinitely quickly with time, Eq. (1)]. A great deal of effort has gone into rectifying this situation by introducing memory effects in an attempt to reproduce, at least qualitatively, the available far-infrared data as measured and catalogued, for example, by Reid.[31] Another hidden assumption in purely rotational or purely translational equations such as Eq. (1) is that the rotational motion of a molecule may be decoupled from the translation of its own center of mass. Computer simulation has been used[24] to show clearly, and for the first time, that there is a well-defined cross-correlation between molecular rotation and translation for all molecular symmetries. In chiral molecules, the difference in the spectral properties of enantiomers and their racemic mixture may be used in principle as an experimental method of detecting this cross-correlation. McConnell et al.[32] have shown how the simplest diffusional theory increases greatly in complexity when inertial effects are taken into consideration, even in the case $V = 0$, that is, for free diffusion governed by Eq. (1). Inertial effects alone *cannot*, however, explain the basic spectral features of dipolar liquids in the far infrared[5] without consideration of the memory effects incorporated in RMT in continued fraction form. Some simple models of the liquid state such as the Calderwood/Coffey itinerant oscillator[33] are RMT-allowed structures and therefore approximants of the appropriate RMT matrix continued fractions. Other models such as the Brownian motion in N-potential wells[23,26,27] are not allowed by RMT and are not generally descriptive of the molecular liquid state. The decoupling and deexcitation effects discovered recently by computer simulation provide these analytical structures with stringent tests. There is no complete analytical method yet available to describe even in rudimentary terms the detailed statistical cross-correlations[34] between rotation and translation in molecular liquids.

Itinerant oscillator theory is now available in a variety of forms, equivalent to various RMT continued fraction approximants.[6] The analytical theory is reviewed elsewhere in this volume. The original two-dimensional linear itinerant oscillator of Calderwood and Coffey[33] is able to qualitatively reproduce the available far-infrared spectra of molecular liquids[5] by simulating the librational (torsional oscillatory) motion of a caged and diffusing molecule. The equations of this version of the itinerant oscillator are soluble numerically using the RMT Pisa algorithm. The linear limit of the itinerant oscillator (essentially speaking, the limit $\sin\theta = \theta$, where θ is the amplitude of the libration) lends itself to analytical solution as described by Calderwood and Coffey.[33] For the case $\sin\theta \neq \theta$, the itinerant oscillator equations become insoluble analytically but have been solved numerically by Ferrario et al.[25] Evans[35] and Coffey[36] discovered independently a formal identity between the linear, two-dimensional itinerant oscillator and the three-variable Mori theory (a linear limit of RMT) in 1976–1977. This is known now to be an example of the structural constraints which RMT imposes on any mathematical model of the molecular liquid state.

These remarks apply to a molecular ensemble free of strong internal or external fields and associated potential terms V. With the imposition of this extra variable, the challenge to analytical theory becomes more difficult to meet[4] and there is a need for a clear and complementary method of approaching the problem numerically[22] using computer simulation.[14-18]

A. Basic Techniques

The vectorization of computer simulation algorithms for new generations of supercomputers is described by Heyes and Fincham in Vol. 63 of this series. Algorithm descriptions are available in the *Quarterly Review* of the

SERC CCP5 group, and actual listings are available from this group (c/o Daresbury Laboratory of SERC, Warrington, UK). The basic algorithms can be adapted simply for the problem at hand by incorporating an extra torque in the appropriate program loop. The torque may be applied to all or some of the molecules used in the simulation. The technique and first results are described in a series of five papers by Evans,[14-18] and this section and the following are based on these articles. These methods of computer simulation are used now for the description of problems of industrial importance, such as Josephson junction hysteresis,[26] nonlinear phenomena in advanced computer circuitry, or soliton diffusion in activated polymers.

The liquid phase of molecular matter is usually isotropic at equilibrium but becomes birefringent in response to an externally applied torque. The computer can be used to simulate (1) the development of this birefringence —the rise transient; (2) the properties of the liquid at equilibrium under the influence of an arbitrarily strong torque; and (3) the return to equilibrium when the torques are removed instantaneously—the fall transient. Evans initially considered[14] the general case of the asymmetric top (C_{2v} symmetry) diffusing in three-dimensional space and made no assumptions about the nature of the rotational and translational motion other than those inherent in the simulation technique itself. A sample of 108 such molecules was taken, each molecule's orientation described by three unit vectors, $\mathbf{e}_A$, $\mathbf{e}_B$, and $\mathbf{e}_C$, parallel to its principal moment-of-inertia axes.

The total thermal energy of the 108 interacting molecules is stabilized by a temperature-rescaling routine written into the program. This is the case with and without an externally applied torque. A uniaxial external force $\mathbf{F}$ is applied to each molecule generating a torque $-\mathbf{e}_B \times \mathbf{F}$ via the arm $\mathbf{e}_B$ embedded in the molecule. The direction $\mathbf{e}_B$ is chosen for convenience and need not be along an axis of the principal moment-of-inertia frame. The torque therefore takes effect in the laboratory frame in a direction mutually orthogonal to $\mathbf{e}_B$ and $\mathbf{F}$ with a magnitude $|\mathbf{e}_B||F|\sin\theta$, where θ is the angle between $\mathbf{e}_B$ and $\mathbf{F}$ for each of the 108 molecules. If $\mathbf{F}$ is the force due to an electric field, then a torque of this kind would be generated from a molecular dipole unit vector coincident with $\mathbf{e}_B$. In general, $\mathbf{F}$ can be an electric, magnetic, electromagnetic, or other type of force field. The computer simulation method is then used to investigate the response of the molecular liquid sample to this field of force. This response can be measured in a number of ways:

1. *Through time autocorrelation and cross-correlation functions at equilibrium.* These can be computed for and among a variety of vectors associated with the molecular motion. They are equilibrium properties, and the fluctuation-dissipation theorem relates them to transient properties such as

$\Delta n(t)/n$, the transiently induced birefringence. By this means, *deterministic* equations of motion, without stochastic terms, can be used via computer simulation to produce spectral features. As we have seen, a stochastic equation such as Eq. (1) is based on assumptions which are supported neither by spectral analysis nor by computer simulation of free molecular diffusion. The field-on simulation allows us the direct use of more realistic functions for the description of intermolecular interaction than any diffusional equation which uses stochastically generated intermolecular force fields.

The time autocorrelation functions of primary interest to the various spectroscopic probes now available are the orientational acf's, for example,

$$\langle P_1(t)\rangle = \langle \mathbf{e}_B(t)\cdot\mathbf{e}_B(0)\rangle$$

$$\langle P_2(t)\rangle = \tfrac{1}{2}\left[3\langle \mathbf{e}_B(t)\cdot\mathbf{e}_B(0)\rangle^2 - 1\right]$$

These are nonexponential near the time origin, and these initial oscillations become more pronounced in the torque-on case[14,17] before the acf's settle into the familiar exponential decay. These oscillations are the signature of the far-infrared frequency region whose power absorption coefficient is essentially the Fourier transform of acf's such as $\langle \mathbf{e}_B(t)\cdot\mathbf{e}_B(0)\rangle$. This acf developes oscillations at equilibrium in the torque-on case, which means that the far-infrared spectrum of a molecular liquid subjected to a strong enough force field would sharpen and shift to higher frequencies. If the external torque becomes much larger than the internal (mean intermolecular) torque, the orientational dynamics will become coherent as in an ideal gas. However, the torque-on far-infrared frequency in the liquid is much higher than in the ideal gas at the same temperature. Because of the involvement of the molecular angular velocity $\boldsymbol{\omega}$ in the kinematic equation[5] linking $\dot{\mathbf{e}}_B$ to $\mathbf{e}_B$ [$\dot{\mathbf{e}}_B = \boldsymbol{\omega} \times \mathbf{e}_B$], the far-infrared spectrum is sensitive to the effect of intense external fields and the way in which these reveal some fundamental properties of the molecular liquid state of matter.

The angular velocity and angular momentum acf's themselves are important to any dynamical theory of molecular liquids but are very difficult to extract directly from spectral data. The only reliable method available seems to be spin-rotation nuclear magnetic relaxation. (An approximate method is via Fourier transformation of far-infrared spectra.) The simulated torque-on acf's in this case become considerably more oscillatory, and, *which is important*, the envelope of its decay becomes longer-lived as the field strength increases. This is dealt with analytically in Section III. In this case, computer simulation is particularly useful because it may be used to complement the analytical theory in its search for the forest among the trees. Results such as these for autocorrelation functions therefore supplement our

analytical knowledge of liquid-phase anisotropy. They are not concerned primarily with reproducing any experimental data which may be available but with simulation of some functions more or less fundamental to the evaluation of the ideas embodied in Eq. (1) and its descendants. The computer enables us to use an external torque of arbitrary strength and origin with a minimum of mathematical elaboration. The most intense field strengths are probably electromagnetic in nature, and an obvious target for computer simulation would be laser-induced far-infrared absorption and dispersion anisotropy.

2. *Through monitoring rise and fall transients.* The simulation is intended to reproduce the conditions under which the linear equation (1) is no longer valid.

Another advantage of the simulation is its ability to make direct tests on the range of validity of basic thermodynamical theorems such as the fluctuation-dissipation theorem. In the second paper of the series by Evans,[15] he considers these points for the simplest type of torque mentioned above, $-\mathbf{e}_B \times \mathbf{F}$. Consider the return to equilibrium of a dynamical variable A after taking off at $t = 0$ the constant torque applied prior to this instant in time. If the torque is removed instantaneously, the first fluctuation-dissipation theorem implies that the normalized fall transient will decay with the same dependence as the autocorrelation function $\langle A(t)A(0)\rangle - A_{eq}^2 / \langle A^2(0)\rangle - A_{eq}^2$. Therefore,

$$\frac{\langle A(t)\rangle - A_{eq}}{\langle A(0)\rangle - A_{eq}} = \frac{\langle A(t)A(0)\rangle - A_{eq}^2}{\langle A^2(0)\rangle - A_{eq}^2}$$

where A_{eq} is the equilibrium average value as $t \to \infty$ after the arbitrary initial $t = 0$.

Theories by Coffey et al.,[3,4] Morita et al.,[2] and Grigolini et al.[22] are available that link the properties of rise and fall transients from stochastic equations of molecular diffusion. In particular, Coffey has shown[4-6] that the Debye diffusion equation produces, in general, rise and fall transients which are dependent on the external field strength and duration. The computer simulation shows clearly[15] that the fluctuation-dissipation theorem becomes inapplicable as the applied field strength increases. Fall transients such as $\langle e_{BZ}\rangle$ decay faster than the equilibrium correlation function $\langle \mathbf{e}_B(t)\cdot\mathbf{e}_B(0)\rangle$. The transient is a simple average over 108 molecules which is equivalent to making the usual single-molecule thermodynamic average in the limit $t \to \infty$ of the transient. Similarly, the transient average $[3\langle e_{BZ}(t)e_{BZ}(t)\rangle - 1]/[3\langle e_{BZ}(0)e_{BZ}(0)\rangle - 1]$ decays more quickly than the equilibrium-averaged autocorrelation function $\{3[\langle \mathbf{e}_B(t)\cdot\mathbf{e}_B(0)\rangle]^2 - 1\}/\{3[\langle \mathbf{e}_B(0)\cdot\mathbf{e}_B(0)\rangle]^2 - 1\}$.

This is the first problem, therefore, to be tackled by the analytical approach and is a fundamental hurdle to be overcome when dealing with data which is in any sense nonlinear. Indeed the RMT structure built up by Grigolini and coworkers implies rigorously and generally that the rules governing molecular diffusion are nonlinear in many interesting and different ways. If the Langevin equation becomes *nonlinear* in *the friction term*, the transient falls away more quickly than the equilibrium autocorrelation function.[6,22] This type of nonlinearity automatically takes care of the other features of the computer simulation, such as non-Markovian and non-Gaussian statistics.

The results of analytical theory are expressed essentially as averages of the type $\langle A^n\rangle$, where A is a dynamical vector, usually an orientation axis of the molecule in which there is embedded a unit vector such as $\mathbf{e}_B$.

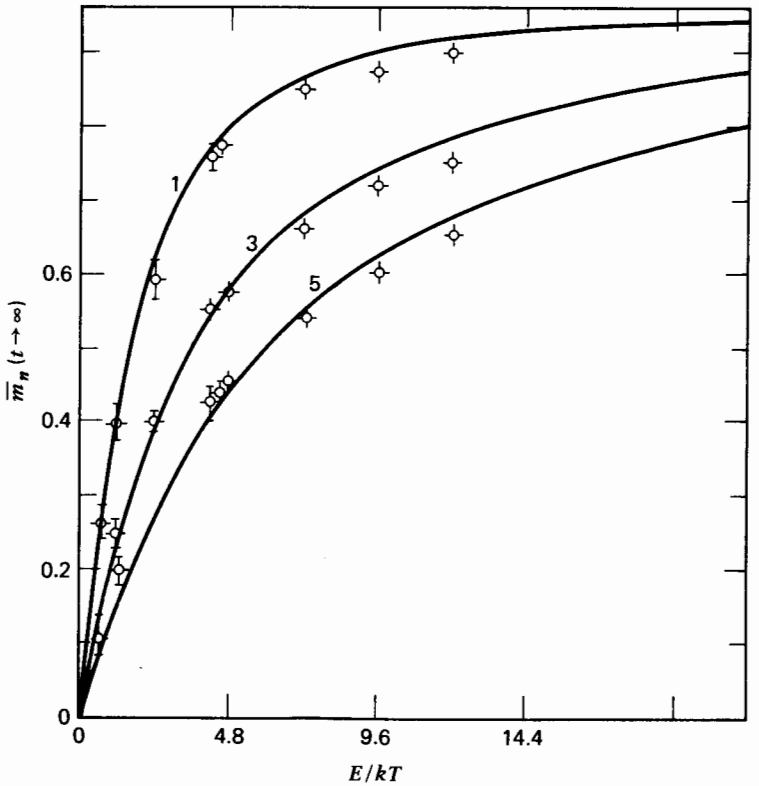

Figure 1. First-, third-, and fifth-order Langevin functions from computer simulation. [Reproduced by permission from *J. Chem. Phys.*, **76**, 5482 (1982).]

This orientation is defined with respect to the static, laboratory frame of reference. Using stochastic concepts, these averages may be derived for positive integral n. The computer simulation allows the calculation of rise and fall transients such as $\langle e_{BZ}^n \rangle$, and this was carried through by Evans[15] for $n=1$ to 6. The simulated rise and fall transients for $\langle e_{BZ} \rangle (n=1)$ are not mirror images, the fall transients being the longer-lived and, in common with the equilibrium acf of $\mathbf{e}_B$, nonexponential. The transient curves are not as smooth as the acf's because in the former case $\langle\ \rangle$ means an average over the 108 molecules only, and in the latter a standard running time average. Therefore, the short-time oscillation in the rise transient may be different for different square-wave field amplitude and duration. The final levels attained by the simulated rise transients as $t \to \infty$ depend on the field strength and duration, as first predicted by Coffey. If, for example, $\langle e_{BZ} \rangle_{t \to \infty}$ is plotted against E/kT, where E is the perturbation energy (Fig. 1), we obtain the Langevin function $L(\mu F/kT)$, where μF is the effective energy due to the

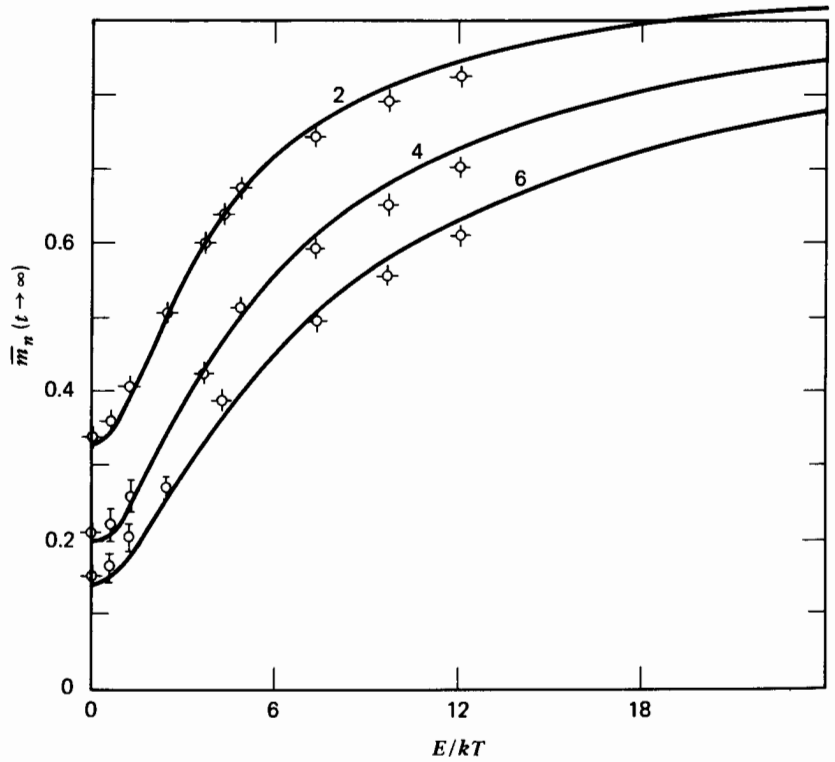

Figure 2. Second-, fourth-, and sixth-order Langevin functions from computer simulation. [Reproduced by permission from *J. Chem. Phys.*, **76**, 5482 (1982).]

applied torque and kT is the mean thermal energy. Similarly, as n is increased from 1 to 6, similar higher-order Langevin functions are obtained from the simulation (Fig. 2). Their self-consistency was checked by Evans,[14] using a nonlinear least mean squares fitting routine to match the *complete set* of computer simulation data to form $L_n(a)$, where L_n denotes the Langevin function of order n:

$$L_1(a) = \frac{e^a + e^{-a}}{e^a - e^{-a}} - \frac{1}{a}$$

$$L_2(a) = 1 - \frac{2L_1(a)}{a}$$

$$L_3(a) = \frac{e^a + e^{-a}}{e^a - e^{-a}} - \frac{3}{a}L_2(a)$$

$$L_4(a) = 1 - \frac{4}{a}L_3(a)$$

$$L_5(a) = \frac{e^a + e^{-a}}{e^a - e^{-a}} - \frac{5}{a}L_4(a)$$

$$L_6(a) = 1 - \frac{6}{a}L_5(a)$$

Obviously, at a given field strength, the same value of a should and does come out of fitting all six computer-generated $\langle e_{BZ}^n \rangle$. This is a good check of the consistency of the computer simulation method, and it would be interesting to make further computations along these lines with different types and durations of external force fields.

1. *Polarizability and Hyperpolarizability*

If an externally applied dielectric field is strong enough, each molecule is distorted in such a way that the effective arm (the total dipole moment) must be described as

$$\mathbf{m} = \boldsymbol{\mu} + \boldsymbol{\alpha} \cdot \mathbf{E}_0 + \tfrac{1}{2}\boldsymbol{\beta} : \mathbf{E}_0\mathbf{E}_0 + \tfrac{1}{6}\boldsymbol{\gamma} : \mathbf{E}_0\mathbf{E}_0\mathbf{E}_0 + \cdots \tag{5}$$

where $\boldsymbol{\mu}$ is the field-off (permanent) dipole moment, $\boldsymbol{\alpha}$ the polarizability, $\boldsymbol{\beta}$ the second, and so on. Here $\mathbf{E}_0$ is the applied electric field. The torque on each molecule is then $\mathbf{m} \times \mathbf{E}_0$. If $\mathbf{E}_0$ is not very large, then in energetic terms the $\boldsymbol{\mu}$ part of the right-hand side of (5) predominates. In condensed phases of matter, where the interaction of molecules is the important feature, $\mathbf{m}$ is supplemented by terms arising from the fields of other molecules, and the

internal field $\mathbf{E}(t)$ at any molecule at a given t is different from $\mathbf{E}_0$. The field $\mathbf{E}(t)$ fluctuates with time, and therefore so does $\mathbf{m}$.

The fourth article of the series considers[18] the development of liquid anisotropy with a torque of the form $(\boldsymbol{\alpha}\cdot\mathbf{E}_0)\times\mathbf{E}_0$ and the field dependence of the relevant order parameters $\langle e_{AZ}^{2n}\rangle$ on E_Z^2. Here E_Z is the Z component of $\mathbf{E}_0$ in the laboratory frame. The angled brackets $\langle\ \rangle$ denote a simple arithmetic average over 108 molecules. The problem in molecular polarizability of non-pair-additive interaction is avoided because of its huge complexity and secondary importance in this context.

In the simplest case this kind of torque may be written in the form

$$-E_Z^2(\alpha_2-\alpha_1)\sin\theta\cos\theta\,\mathbf{u} \tag{6}$$

where θ is the angle between the field direction Z and $\mathbf{e}_A$ is a unit vector in the A axis of the principal moment of inertia frame. α_1 and α_2 are components of the molecular polarizability tensor along and perpendicular to $\mathbf{e}_A$. It is assumed for simplicity's sake that the two components of α perpendicular to $\mathbf{e}_A$ are equal. Here $\mathbf{u}$ is a unit vector defining the direction of the imposed torque. By definition

$$\cos\theta=\frac{\mathbf{e}_A\cdot\mathbf{E}_0}{|\mathbf{e}_A||\mathbf{E}_0}=\frac{e_{AZ}E_Z}{|\mathbf{E}_0|}=e_{AZ}$$

$$\sin\theta\mathbf{u}=\frac{\mathbf{e}_A\times\mathbf{E}_0}{|\mathbf{e}_A||\mathbf{E}_0}=\mathbf{i}e_{AY}-\mathbf{j}e_{AX}$$

where $\mathbf{i}$ and $\mathbf{j}$ are unit vectors. Therefore, the torque is

$$-E_Z^2(\alpha_2-\alpha_1)(\mathbf{i}e_{AZ}e_{AY}-\mathbf{j}e_{AZ}e_{AX}) \tag{7}$$

for each molecule at each instant t. Here $\mathbf{i}$ is a unit vector in the X direction. Clearly, the elements of Eq. (7) are defined in the static (laboratory) frame of reference.

Kielich[37] has calculated the "Langevin functions" generated by this type of torque, where $\mathbf{E}_0$ is an electric field. The torque produces the results

$$\langle e_{AZ}^{2n+1}\rangle=0$$

for positive integral n, that is, its effect is detectable only through even-order averages over $\langle e_{AZ}^{2n}\rangle$. The computer simulation, to be valid, must therefore reproduce these features exactly. Defining $q=(\alpha_2-\alpha_1)E_Z^2/2kT$, Kielich

produces ($q=|q|$)

$$L_1(\pm q)=0$$

$$L_2(\pm q)=+\frac{1}{2q}\pm\frac{1}{2q^{1/2}I(\pm q)}$$

$$L_3(\pm q)=0$$

$$L_4(\pm q)=\frac{3}{4q^2}\pm\frac{2q+3}{4q^{3/2}I(\pm q)}$$

$$I(\pm q)=e^{\mp q}\int_0^{\sqrt{q}}e^{\pm x^2}\,dx$$

so that $L_1(\pm q)$ describes the q dependence of $\langle e_{AZ}\rangle$, $L_2(\pm q)$ that of $\langle e_{AZ}^2\rangle$, and so on. For small values of q,

$$L_2(\pm q)=\tfrac{1}{3}\pm\frac{4q}{45}+\frac{8q^2}{945}\pm\frac{16q^3}{14175}+\cdots$$

$$L_4(\pm q)=\tfrac{1}{5}+\frac{8q}{105}+\frac{16q^2}{1575}\mp\frac{32q^3}{51975}-\cdots$$

As $E_Z\to\infty$, $L_2(+q)\to 1$; and $L_2(-q)\to 0$, as do the L_4 functions. We shall call the L_2 and L_4 functions the second- and fourth-order Kielich functions, respectively.

The great advantage of the computer simulation method is that if it passes the test represented by these analytical results it may be used to investigate the molecular dynamics for all strengths of E_Z without any of the formidable difficulties associated with the stochastic theory, typified in the tours de force by Morita and coworkers.[2] Evans verifies in his article[18] that both second- and fourth-order Kielich functions *can* be generated self-consistently by computer simulation. The method used is analogous to the earlier work on Langevin functions.[14] He then illustrates the power of the computer simulation by investigating the effect of an arbitrarily strong second-order torque on the statistical correlation between a molecule's center-of-mass translational velocity $\mathbf{v}$ and its *own* angular velocity $\boldsymbol{\omega}$ an interval t later in time. The computations are carried out for an asymmetric top diffusing in three dimensions. It is possible to quantify this correlation [which invalidates the Langevin equation (1)] only in a *moving* frame of reference. This may be illustrated with the following frame transformation. Let v_X, v_Y, and v_Z be the components of $\mathbf{v}$ in the laboratory frame (X, Y, Z). Define a moving (molecular) frame of reference with respect to unit vectors $\mathbf{e}_A$, $\mathbf{e}_B$, and $\mathbf{e}_C$ along the principal moment-of-inertia axes of the molecule under considera-

tion. The components of $\mathbf{v}$ in the moving frame of the principal moments of inertia are then

$$v_A = v_X e_{AX} + v_Y e_{AY} + v_Z e_{AZ}$$
$$v_B = v_X e_{BX} + v_Y e_{BY} + v_Z e_{BZ}$$
$$v_C = v_X e_{CX} + v_Y e_{CY} + v_Z e_{CZ}$$

and similarly for $\boldsymbol{\omega}$. By applying symmetry rules of parity, time reversal, and so on, to our C_{2V}-symmetry molecule, we deduce that the cross-correlation function elements

$$\langle v_C(t)\omega_B(0)\rangle \quad \text{and} \quad \langle v_B(t)\omega_C(0)\rangle$$

exist for $t > 0$. All others vanish for all t. Both these functions exist at equilibrium in the molecular ensemble in the presence *and* absence of the external force field. In the latter case, both first-order correlation functions oscillate, the (C, B) function attaining[18] a maximum of $+0.22$ and a minimum of -0.04 with an uncertainty of ± 0.01 or thereabouts. It is clear, therefore, even *before* applying our field, that the classical theory of rotational Brownian motion, so long accepted as the basis of subjects such as dielectric relaxation, cannot be used to describe these rototranslational signatures. These respond to a field corresponding to $q = 17.5$ by becoming more oscillatory, the (CB) element this time having a positive peak of $+0.12$ and a negative peak of -0.13. If we take into consideration the fact that cooperativity in, for example, a mesophase is known to magnify single-molecule properties enormously (e.g., the Kerr constant[37] $\to \infty$) is is likely that rototranslation is the key to explaining many of the spectral features observable in the aligned (or unaligned) mesophase. First-order mixed autocorrelation functions of linear and angular velocity vanish for all t in the *laboratory* frame (X, Y, Z) for achiral molecular symmetries. For this reason, they have eluded detection until the recent suggestion to use moving frames by Ryckaert and coworkers.[39] The parity rule does *not* imply that the effects of rototranslation can be ignored. On the contrary, they are critically important and underpin every type of spectrum whose origins can be traced to molecular diffusion.[5,6] With the use of electric, and probably magnetic, fields, first-order linear, angular velocity acf's become observable in the laboratory frame. This has been confirmed recently by computer simulation (unpublished work).

B. Nonlinear Molecular Dynamics under Intense Force Fields

These dynamics are investigated in detail in the fifth part of the series.[17] This article was intended to pave the way numerically for future advances in the analytical theory of nonlinear molecular dynamics. The simplest type of

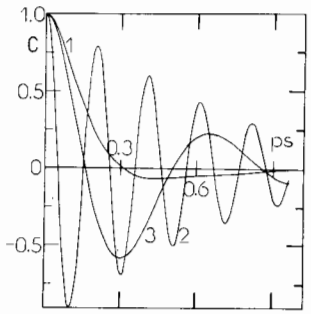

Figure 3. High-field components of the angular velocity acf. [Reproduced by permission from *J. Chem. Phys.*, **78**, 925 (1983).]

torque $(-\mathbf{e}_A \times \mathbf{F})$ is used to produce a variety of auto- and cross-correlation functions in the laboratory and moving frames of reference. In this section we describe briefly the features that emerge from the numerical analysis.

1. The velocity and angular velocity autocorrelation functions become more oscillatory as the externally applied torque increases in strength (Fig 3). Moving-frame component acf's such as $\langle v_A(t)v_A(0)\rangle/\langle v_A^2\rangle$ have different time dependencies, that is, $\langle v_A(t)v_A(0)\rangle/\langle v_A^2\rangle \neq \langle v_B(t)v_B(0)\rangle/\langle v_B^2\rangle \neq \langle v_C(t)v_C(0)\rangle/\langle v_C^2\rangle$, and so on, and the differences become more pronounced as the torque increases. Cross-correlation functions such as $\langle v_C(t)\omega_B(0)\rangle$ or $\langle \omega_C(t)v_B(0)\rangle$ become more oscillatory as the field strength increases to saturation level (about $34kT$).
2. The statistics governing the evolution of the center-of-mass velocity are not Gaussian. This is revealed by an examination of the kinetic energy acf $\langle v^2(t)v^2(0)\rangle/\langle v^4(0)\rangle$, which is invariant to frame transformation. The computer simulation produces accurately the $t \to \infty$ limit $(\frac{3}{5})$ of this acf even in the presence of a very strong field, energetically equivalent to $35.0kT$. In the interval between $t = 0$ and $t \to \infty$, the kinetic energy acf is different from the theoretical curve from Gaussian statistics. One of the interesting side effects of nonlinear RMT is its ability to reproduce this behavior analytically as described by Grigolini in the opening chapter of this volume.
3. The rotational velocity acf becomes rapidly oscillatory under a $35kT$ field. This means the *far-infrared absorption*[5] would be shifted to higher frequencies and sharpened considerably (Fig. 4).
4. The field-on angular velocity and angular momentum acf's in the laboratory frame are oscillatory, and the envelope of the decay of these oscillations becomes field-dependent as mentioned already.

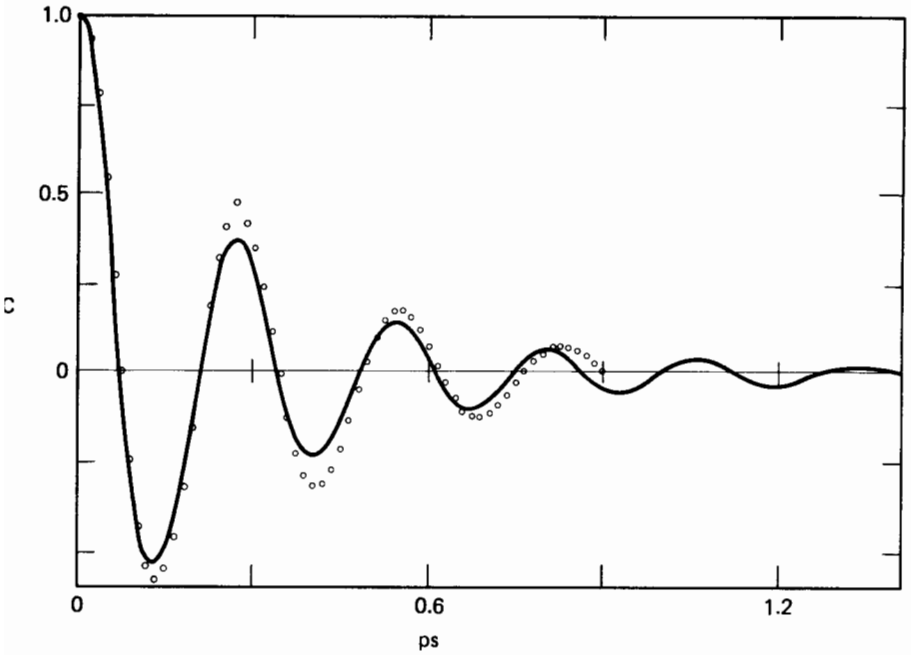

Figure 4. Rotational velocity (—) and angular velocity (O) a.c.f.'s under the influence of a strong external field. [Reproduced by permission from *J. Chem. Phys.*, **78**, 925 (1983).]

This "decoupling" effect[17] verifies Grigolini's prediction[9] of 1976 made in the context of vibrational relaxation[19,20] using RMT.

C. Transients Induced by Alternating Fields

Finally, we mention the results of article three[16] in the series, which considers an alternating external field $F = F_0 \cos \omega t$. The theory, for example, of the Kerr effect in an alternating electric field is confined to the case where the field is weak and has been reviewed by Kielich.[37] Two processes have been identified according to the value of ω.

1. If ω is much smaller than the characteristic frequency ω_0 of oscillations of the molecule, the field will have a reorienting effect, causing some polarization in the medium. If the oscillating, orienting field is made stronger, this polarization effect approaches saturation, and linear response theory is no longer applicable.
2. If ω is much higher than ω_0, no orientation of the electric dipoles is possible, and its only effect is electron distortion within each molecule.

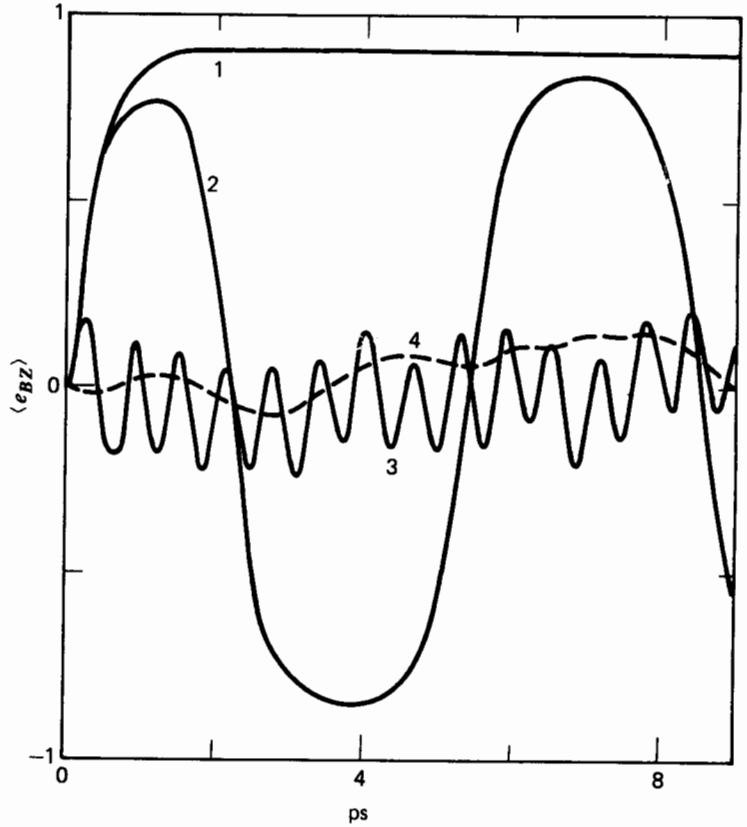

Figure 5. Dispersion of the rise transients induced with an alternating field of increasing frequency (lowest frequency, curve 1). [Reproduced by permission from *J. Chem. Phys.*, **77**, 4632 (1982).]

The computer can be used to investigate in detail phenomena 1 and 2, which represent a dispersion of the rise transient for a given field strength as the frequency increases. Results were obtained[16] for $\omega = 0$, 10^{12}, 10^{13}, and 10^{14} radians per second, frequencies which take us through the dispersion region because the molecular dynamics simulation takes place on a picosecond time scale. In the static field ($\omega = 0$) we observe a conventional rise transient (Fig. 5). In an alternating field at frequencies below about 10^{11} rad/s, the plateau value of this transient is reached periodically as the external field reverses direction. However, as the alternating field frequency approaches the far-infrared/microwave region, the movement of the molecules in response to the strong external alternating field of force produces a transient which becomes rapidly oscillatory but which fails to reach the plateau

level imposed by the static external field. In other words, the transient response is dispersed.

The form taken by each transient is the result of competition between the aligning field and the thermal opposition. The transient oscillations are not simple and are relatively long-lived in comparison with the rise time in the static field. The amplitude of the transient decreases (as mentioned already) as the field frequency increases, but even at $\omega = 10^{14}$ rad/s a long-lived response is measurable above the noise of the computer simulation.

The higher order transients $\langle e_{BZ}^n \rangle$ $(n = 2,3,\ldots)$ are of interest in the theory of the Kerr effect, depolarized light scattering from birefringent liquids, spin-spin NMR, incoherent inelastic scattering, and so on. The mean value of $\langle e_{BZ}^2 \rangle$ from the simulation is shifted upwards from $\frac{1}{3}$ (the $t = 0$ value) by the alternating field. The mean value of $\langle e_{BZ} \rangle$, on the other hand, is very small, although the amplitude of the oscillations in this function is much larger. This suggests that only second-order transients (or even-order transients) produce birefringence in an achiral molecular liquid subjected to an alternating field (e.g., an electromagnetic field). This is the case experimentally in laser-induced birefringence when the molecules are achiral.

The external field used in this type of simulation breaks time-reversal symmetry, and a magnetic field would break parity-reversal symmetry. Lorentz forces on partial charges located on atoms of each molecule would make the latter precess along the magnetic field pseudo-vector. It is expected that a simulation of such a system would produce insight into new couplings via nonvanishing mixed autocorrelation functions such as the moving-frame functions described already (see Section IV).

A clue to the analytical understanding of these numerical results comes from the fact that the amplitude of the transients for high ω appears to be random. This could be accounted for by a theory based on amplitude randomness in an externally driven pendulum system.[4,6]

III. ANALYSIS OF THE NUMERICAL DATA WITH RMT

A. The Decoupling Effect

The nature of the excitation has a profound influence on the subsequent relaxation of molecular liquid systems, as the molecular dynamics simulations show. This influence can be exerted at field-on equilibrium and in decay transients (the deexcitation effect). Grigolini has shown that the effect of high-intensity excitation is to slow the time decay of the envelope of such oscillatory functions as the angular velocity autocorrelation function.[5] The effect of high-intensity pulses is the same as that of ultrafast (subpicosecond laser) pulses. The computer simulation by Abbot and Oxtoby[40] shows that

in vibrational relaxation an increase in the time duration of the exciting pulses marks the oscillatory decay behavior of highly non-Markovian systems, that is, those in which memory effects are important. These results have been explained analytically by Grigolini, using RMT as described in this section in the related context of rototranslational relaxation of molecular liquids in the presence of very strong external fields. Some further evidence for the validity of Grigolini's RMT has been put forward by Bagchi and Oxtoby,[19,10] using Monte Carlo methods.

Both vibrational and rotovibrational relaxation can be described analytically as multiplicative stochastic processes. For these processes, RMT is equivalent to the stochastic Liouville equation of Kubo,[41] with the added feature that RMT takes into account the back-reaction from the molecule under consideration on the thermal bath. The stochastic Liouville equation has been used successfully to describe decoupling in the transient field-on condition[5] and the effect of preparation on decay.[19,20,42] When dealing with liquid-state molecular dynamics, RMT provides a rigorous justification for itinerant oscillator theory,[25,33] widely applied to experimental data by Evans and coworkers.[5,31] This implies analytically that decoupling effects should be exhibited in molecular liquids treated with strong fields. In the absence of experimental data, the computer runs described earlier[14-18] amount to an independent means of verifying Grigolini's predictions. In this context note that the simulation of Oxtoby and coworkers[19,20] are "semistochastic" and serve a similar purpose.

1. *Decoupling Effects in the Quasi-Markov Limit*

The simplest RMT structure needed to describe field-on computer simulations[17] is the essentially two-dimensional equation

$$\frac{dC(t)}{dt} = -\int_0^t \phi(t-\tau)C(\tau)\,d\tau + i\omega_1 C(t) \tag{8}$$

with frequency $\omega_1 = (\mu E/I)^{1/2}$, where μ and I denote the dipole and the moment of inertia, respectively, of a given molecule. This describes a torque applied externally, as in the simulation, to each molecule of the sample.

Equation (8) can be rewritten as

$$\frac{d\tilde{C}(t)}{dt} = -\int_0^t \exp[-i(t-\tau)\omega_1]\,\phi(t-\tau)\tilde{C}(\tau)\,d\tau \tag{9}$$

with the autocorrelation function written in the "interaction picture" as

$$\tilde{C}(t) = \exp[i\omega_1 t]C(t) \tag{10}$$

Assume, for the memory function, that

$$\phi(t) = \phi_0 \exp(-\gamma_a t) \tag{11}$$

with γ_a large enough to approach the Markov limit for $C(t)$, that is, with the $\phi(t)$ a quasi-delta function in time. This implies in the original frame of reference that

$$\frac{dC(t)}{dt} = [i\Omega(\omega_1) - \Gamma(\omega_1)]C(t) \tag{12}$$

where

$$\Omega(\omega_1) = \omega_1 + \frac{\omega_1 \phi_0}{\omega_1^2 + \gamma_a^2} \tag{13}$$

$$\Gamma(\omega_1) = \frac{\gamma_a \phi_0}{\gamma_a^2 + \omega_1^2} \tag{14}$$

For finite γ_a, the decay of the oscillation envelope becomes slower as the frequency ω_1 increases. This is the Grigolini decoupling effect in its simplest form and is qualitatively in agreement[21] with the computer simulations of Section II. *Note that there is no decoupling effect in Markovian systems*[23] (i.e., those where $\gamma_a \to \infty$).

When the system under consideration becomes significantly non-Markovian, we have to release the implicit assumption that the memory kernel is unaffected by external excitation. The three-dimensional computer simulation[14] of dichloromethane of Section II is described, for simplicity, with a liquid sample consisting of disks with moment of inertia I constrained to move on a plane surface and colliding with each other. Each disk has an electric dipole μ in one of its diameters. Using the Mori basis set provides the equation of motion:

$$\frac{d\theta}{dt} = iL_0\theta \tag{15}$$

where θ is the orientation angle of the tagged molecule and L_0 is the

Liouvillian of the model system. This can be approximated by

$$\begin{aligned} \frac{df_0}{dt} &= f_1 \\ \frac{df_1}{dt} &= -\Delta_0^2 f_0 + f_2 \\ \frac{df_2}{dt} &= -\Delta_1^2 f_1 + f_3 \\ \frac{df_3}{dt} &= -\Delta_2^2 f_2 - \gamma f_3 + F(t) \end{aligned} \tag{16}$$

where $f_0 \equiv \theta$, $f_1 \equiv \omega \equiv \dot{\theta}$. In the absence of an external field, $\Delta_0 = 0$. In the presence of the field we have to add to iL_0 the following interaction:

$$\mathscr{L}_1 \equiv iL_1 = -\left(\frac{E\mu}{I}\right)\sum_i \sin\theta_i \doteq -\omega_1^2 \sum_i \theta_i \tag{17}$$

θ is the angle between the ith dipole and the direction of the electric field. The linear approximation is justified when $\langle \omega^2 \rangle \ll \omega_1^2$.

The dynamics of an infinite chain of states is simulated by the friction γ and stochastic force $F(t)$ in the final equation of set (16). If these dynamics involve frequencies much higher than ω_1, that is, if they occur on a very much faster time scale, the expansion of L_1 can be limited to the four equations of set (16), assuming that γ and F are unaffected by the field. With these assumptions, Eq. (16) is equivalent to the model of the itinerant oscillator:[33]

$$\begin{aligned} \dot{\theta} &= \omega \\ \dot{\omega} &= -\Delta_1^2(\theta - \psi) - \omega_1^2\theta \\ \dot{\psi} &= \nu \\ \dot{\nu} &= \Delta_2^2(\theta - \psi) - \omega_2^2\psi - \gamma\nu + f(t) \end{aligned} \tag{18}$$

When $\gamma \gg \Delta_2$ the equivalent of the microscopic time γ_a^{-1} is $\Gamma^{-1} \equiv \gamma/\Delta_2^2$. Decoupling effects are present when $\omega_1 \doteq \Gamma$. To obtain an approximate value of Γ we can use the experimental data as follows. First, we evaluate the value of decay of the oscillation envelopes of the angular velocity autocorrelation function as a function of ω_1. Equation (14) shows that this is, approximately, a Lorentzian, the linewidth of which provides the approximate expression for Γ. The agreement with the numerical decoupling effect is quantitatively good[21] when the ratio ω_2^2/ω_1^2 is assumed to be equal to 8.5. Simple Markovian models cannot account for decoupling effects.

B. Deexcitation Effects

These simulations test the basic validity of the fluctuation-dissipation theorem:

$$\Delta_A(t) = C_A(t) \tag{19}$$

where

$$\Delta_A(t) = \frac{\langle A(t)\rangle}{\langle A(0)\rangle} \tag{20}$$

$$C_A(t) = \frac{\langle A(t)A(0)\rangle_{eq}}{\langle A^2\rangle_{eq}} \tag{21}$$

The autocorrelation function $C_A(t)$ is evaluated at equilibrium, whereas $\Delta_A(t)$ is a transient property requiring preliminary excitation of the variable of interest A. Evans investigated this problem by monitoring via computer simulation[15] the time behavior of a liquid sample after the instantaneous removal of a strong external field of force **E**. He found that at the point $\mu E/kT = 12$, $\Delta_A(t)$ decays considerably faster than $C_A(t)$. Here μ is the dipole of the tagged molecule and μE is the energy associated with the field of force **E**. In that case A is the component of the dipole along the Z axis.

1. *Linear and Nonlinear Systems Far from Equilibrium*

Under a wide range of conditions (described elsewhere in this volume), the fundamental equation of motion

$$\frac{dA}{dt} = iLA \tag{22}$$

can be recast in the general form[44,45]

$$\frac{dA}{dt} = \lambda A - \int_0^t \phi_A(t-\tau)A(\tau)\,d\tau + F_A(t) \tag{23}$$

Assuming that the stochastic force vanishes on average:

$$\langle F_A(t)\rangle = 0 \tag{24}$$

By a simple Laplace transform, from Eq. (23), we have

$$\Delta_A(t) = \mathscr{F}_A(t) \tag{25}$$

where

$$\mathscr{F}_A(t) = \mathscr{L}_a^{-1}[s - \lambda + \hat{\phi}_A(s)] \tag{26}$$

and $\hat{\phi}_A(s)$ denotes the Laplace transform $\mathscr{L}_a[\phi_A(t)]$. A further basic requirement for Eq. (19) to be valid is that $\phi_A(t)$ is a genuine equilibrium property. Zwanzig[44] has shown that in the nonlinear case the memory function $\phi_A(t)$ also depends on the variable of interest A. This means that if we excite that variable, we can destroy the basic condition that $\phi_A(t)$ must be a genuine equilibrium property. This prevents $\Delta_A(t)$ from being identifiable with the equilibrium property $C_A(t)$, as implied by the fluctuation-dissipation theorem.

The fundamental reason why excitation has an influence on the decay process is the breakdown of condition (24). This has profound consequences on relaxation when the time scale of the stochastic force $F_A(t)$ is not well separated from that of the variable of interest A, that is, when memory effects are important. The deexcitation effect is a direct consequence of the invalidation of Eq. (24) by intense external force fields and was first investigated by Grigolini and coworkers following the computer simulations described in Section II.

The preparation effect which results in the breakdown of Eq. (24) is relevant only when considering the intense non-Markovian case of Section II (even in the linear case). A review of these effects can be found in ref. 7.

When dealing with a nonlinear case, even when a large time scale separation between the system of interest and thermal bath is available, a new preparation effect takes place related to the fact that the memory kernel Φ_A depends on excitation.

The argument by Zwanzig links the violation of condition (24) with a well-defined nonlinearity in the stochastic equations describing the system under consideration (an ensemble of molecules). One way of introducing this type of nonlinearity is to use the nonlinear itinerant oscillator

$$\begin{aligned}
\dot{\theta} &= \omega \\
\dot{\omega} &= -\kappa \sin[N(\theta - \psi + \xi)] - \omega_1^2 \sin\theta \\
\dot{\psi} &= \nu \\
\dot{\nu} &= \kappa \sin[N(\theta - \psi + \xi)] - \omega_2^2 \sin\psi - \Gamma_\nu \nu + f(t)
\end{aligned} \tag{27}$$

The derivation of these equations is described elsewhere in this volume. ξ is the average value of the angle between real and "virtual" dipole *when no external field is present.*

To simplify the calculation, Grigolini assumed[22] ν to be an infinitely fast variable, thereby providing

$$\begin{aligned}
\dot{\theta} &= \omega \\
\dot{\omega} &= -\kappa \sin(N\Delta) - \omega_1^2 \sin\theta \\
\dot{\Delta} &= -\frac{\kappa}{\Gamma_\nu}\sin(N\Delta) + \omega \\
&\quad -\frac{\omega_2^2}{\Gamma_\nu}\sin[N(\theta+\xi-\Delta)] + \frac{f(t)}{\Gamma_\nu} \\
\Delta &= \theta - \psi + \xi
\end{aligned} \tag{28}$$

which is the nonlinear extension of the equivalent second-order Mori approximant discussed by Berne and Harp.[46] In the absence of an external field, a simplified picture approximately equivalent to Eq. (28) can be obtained, provided Δ is must higher in frequency than ω. This assumption allows the use of the adiabatic elimination procedure (AEP) developed in Chapter II within the context of RMT. It is then possible to show that the *long-time* behavior of Eq. (28) is roughly equivalent to that provided by the following Markovian, but nonlinear, equation:[47-49]

$$\dot{\omega} = -\gamma\omega + \gamma'\omega^3 + F(t) \tag{29}$$

where

$$\gamma = \kappa N \frac{\langle\cos(N\Delta)\rangle}{\Gamma}$$

$$\gamma' = \frac{\kappa N^3}{6}\frac{\langle\cos(N\Delta)\rangle}{\Gamma^3}$$

$$\Gamma \equiv \frac{\kappa N}{\Gamma_\nu}$$

Note that this description is qualitatively correct, but flawed. Equation (29) does not satisfy the requirement of canonical equilibrium, and the correction is evaluated via linearization which underestimates the intensity of the correction itself. In Chapter VI a more accurate approach is shown. The arguments of this section are correct only from a qualitative point of view.

The details of how $F(t)$ is related to $f(t)$ are given elsewhere in this volume. Equation (29) may be used to describe the deexcitation effects described in Section II. A more accurate analytical description is provided by the numerical solution of the set of equations making up the nonlinear itinerant oscillator using continued fraction analysis.

2. *Comparison with Computer Simulation*

Assume that θ is a slow relaxation variable compared with ω. Using the adiabatic elimination procedure (AEP)[47,48] described in Chapter II, we obtain for the probability distribution of the variable θ, $\sigma(\theta; t)$ the following, generally valid, equation of motion:

$$\frac{\partial\sigma(\theta;t)}{\partial t} = \sum_{n=2}^{\infty}\int_0^t ds\,\phi_n(t,s)\frac{\partial^n\sigma(\theta;s)}{\partial\theta^n} \tag{30}$$

This result is obtained by taking into account only the contribution $\mathscr{L}_1^2$ of the theory developed in Chapter II. If θ is almost Markovian, the higher order derivatives are negligible, leaving

$$\frac{\partial\sigma(\theta;t)}{\partial t} = D(t)\frac{\partial^2\sigma(\theta;t)}{\partial\theta^2} \tag{31}$$

where

$$D(t) \equiv \int_0^t ds\left[\langle\omega(t)\omega(s)\rangle - \langle\omega(t)\rangle\langle\omega(s)\rangle\right] \tag{32}$$

Due to the overall symmetry constraints on a nonrotating molecular liquid sample, $\langle\omega(t)\rangle = \langle\omega(s)\rangle = 0$ even in the transient region. It is difficult to evaluate the nonstationary correlation function:

$$\begin{aligned}
\phi(t,\tau) &= \langle\omega(t)\omega(t-\tau)\rangle \\
&\equiv \int d\omega\, d\Delta\left(e^{\Gamma_0^+\tau}\omega\right)\omega\sigma_B(\omega,\Delta;t)
\end{aligned} \tag{33}$$

where Γ_0 is the Fokker-Planck operator of the (ω, Δ) system, and

$$\begin{aligned}
\sigma_B(\omega,\Delta;t) = Ke^{\Gamma_0 t}\int d\theta\exp\Big(\langle\omega^2\rangle_{\text{eq}}^{-1}\Big[&\frac{\kappa}{N}\cos(N\Delta) + \omega_1^2\cos\theta \\
&+ \omega_2^2\cos(\theta+\xi-\Delta) - \tfrac{1}{2}\omega^2\Big]\Big)
\end{aligned} \tag{34}$$

that is, the state of the (ω, Δ) system at a time t far from the sudden removal of the field, K is a suitable normalization factor, and $\langle\omega^2\rangle_{\text{eq}}$ denotes the equilibrium value of $\langle\omega^2\rangle$, which is dependent on whether or not the external field is present.

To evaluate this nonstationary correlation function, we shall assume that the variable ω is much slower than the "virtual" variable Δ. This allows us

to envisage a simplified approach to the evaluation of the transient correlation function of Eq. (33). Soon after the sudden removal of the external field, Δ obtains its equilibrium distribution, thereby determining a change in the ω distribution from the equilibrium state. Neglecting the short-time contribution to $\phi(t,\tau)$, we can write

$$\phi(t,\tau) = K' \int d\omega\, d\Delta \left(e^{\Gamma_0^+ \tau}\omega\right) \omega \exp\left[-\frac{\omega^2}{2}\left\langle \omega^2(0)\right\rangle\right] \sigma_{eq}(\Delta) \tag{35}$$

where K' is a suitable normalization factor, $\sigma_{eq}(\Delta) \propto \exp[k\cos(N\Delta)/N\langle\omega^2\rangle_{eq}]$, and $\langle\omega^2(0)\rangle$ denotes the value of $\langle\omega^2(t)\rangle$ at the time t far from the sudden removal of the external field when this average value attains its largest deviation from $\langle\omega^2\rangle_{eq}$.

It must therefore be understood that this is the new time origin. t is much shorter than the relaxation time of the variable ω. Throughout the analysis of this section, a parameter of basic importance is

$$R \equiv \left\langle \omega^2(0)\right\rangle - \left\langle \omega^2\right\rangle_{eq} \tag{36}$$

The absolute value of this parameter depends strongly on the intensity of the "virtual" dipole. By numerical means, we can show that for positive R', nonvanishing values of ξ are required. This can be understood on physical grounds through the fact that for $\xi = 0$, strong fields do not change the average value of the angle between real and "virtual" dipole, although they prevent large fluctuations about the mean value. The field-on equilibrium distribution is therefore associated with values of the corresponding potential energy smaller than those in the absence of the field. Assuming that $N = 1$, $\xi = \pi$, the effect of strong fields is to reduce the angle between real and "virtual" dipole from π to 0, thereby resulting in an effect which is the reverse of that described above. This makes it possible to obtain positive values for R. A more accurate discussion of this issue will be given in Chapter VI.

Focusing our attention on the slow reequilibrium process of ω, and using the results of AEP, we can derive from Eq. (33) the new equation

$$\phi(t,\tau) = \int d\omega\,\omega \left(e^{\Gamma_{ad}^+ \tau}\omega\right) \exp\left[-\frac{\omega^2}{\left\langle \omega^2(t)\right\rangle}\right] \tag{37}$$

where Γ_{ad} is the effective operator associated with Eq. (37). To evaluate explicitly the time dependence of $\langle\omega^2(t)\rangle$, we can use the following mean field approximation to Eq. (37):

$$\dot{\omega} = -\gamma\omega + \gamma' \left\langle \omega^2(t)\right\rangle \omega + F(t) \tag{38}$$

and solve this equation with the method of Suzuki. This results in

$$\left\langle \omega^2(t)\right\rangle = \frac{\left\langle \omega^2\right\rangle_{eq} + R\left(\gamma + \left\langle \omega^2\right\rangle_{eq}\gamma'\right)e^{-2\gamma' t}/(\gamma - R\gamma')}{1 + R\gamma' e^{-2\gamma' t}/(\gamma - R\gamma')} \tag{39}$$

In strongly nonlinear systems (large γ') and/or with significant excitation (large positive values of R), Eq. (39) locks the process of energy exchange between ω and its thermal bath. *This accelerates the decay of* $\langle\cos\theta(t)\rangle$ *according to Eq.* (31).

Equation (37) gives the result

$$\phi(t,\tau) = \left\langle \omega^2(t)\right\rangle \exp\left[-\left(\gamma - \gamma'\left\langle \omega^2(t)\right\rangle\right)\tau\right] \tag{40}$$

Equations (31) and (32) then result in

$$\left\langle \cos\theta(t)\right\rangle = \exp\left(-\int_0^t D(t')\,dt'\right)\left\langle \cos\theta(0)\right\rangle \tag{41}$$

for the fall transient of $\langle\cos\theta(t)\rangle$, where

$$D(t) = \int_0^t \phi(t,\tau)\,d\tau \tag{42}$$

and $\phi(t,\tau)$ is defined by Eqs. (40) and (41). Note that in the absence of excitation ($R = 0$), Eq. (42) reduces to the well-known Kubo result for the stochastic oscillator.[41] The analytical theory summarized briefly in these equations accounts qualitatively for the numerical deexcitation effect.[22] A quantitative description can be obtained under carefully controlled numerical conditions using the CFP to solve the nonlinear diffusion equations and from a more detailed discussion of the dependence of R on both ω_2 and ξ.

The RMT is a method for finding simplified models that satisfy the rigorous formal constraints imposed by the most general theories of relaxation. The structure of RMT implies that only some models of the liquid state can be accepted. Those that are invalidated by RMT cannot reproduce some basic features such as the deexcitation effect. Numerical methods such as computer simulation are now becoming important in uncovering some basic properties of the liquid state—properties that can be analyzed with RMT. An experiment could be made to detect the deexcitation effect using strong, ultrafast (subpicosecond) laser radiation (e.g., Nd-YAg laser with a streak camera detection system for second-order rise and fall transients).

The formal structure of RMT at short times implies that *dissipative processes cannot affect some variables of interest directly*. In this way it is possible to account for decoupling phenomena described earlier in this review. When the reduced model is given a nonlinear character, the long-time behavior of the corresponding part of interest of the system satisfies the constraints of the rigorous, generally valid, theory of relaxation. *The slowing down of averages associated with* ω, *and therefore the acceleration of the fall transient* $\langle \cos\theta(t) \rangle$, *are both natural outcomes of RMT*. The simplified theory of this section deals with the long-time limit of the more general theory, because in this limit the equations are tractable analytically. The CFP is capable of solving the equations without this constraint. An investigation of the role of the "virtual" dipole is necessary, because the computer simulation of the excitation effect implies that ξ does not vanish, that is, the angle between the real and virtual dipoles does not vanish on average. The theory of this section can be checked by using the CFP which, as shown in Chapter I, stems from the same theoretical background as that behind the RMT.

IV. FIELD EFFECTS IN CHIRAL MOLECULES: COMPUTER SIMULATION

Several interrelated problems in vapor and condensed phase molecular dynamics have been brought together recently using the computer simulation of optically active molecules. It is well known[50] that the average interaction potential between one R enantiomer and another R enantiomer is slightly different from that between R and S enantiomers. This is sometimes described in textbooks and review articles as "chiral discrimination." The effects[51] of chiral discrimination are sometimes very small, because the potential energy difference $\Delta V = V(R\text{-}R) - V(R\text{-}S)$ is only a few calories per mole. Nevertheless, it ought to be detectable spectroscopically with techniques already available such as infrared/radio-frequency double resonance and nonlinear, inverse lamb dip spectroscopy of dilute chiral gases. The effects of chiral discrimination in the Hamiltonian governing the molecular dynamics of a mixture of R and S camphor vapors will result in these types of ultra-high-resolution spectra being clearly different for RS and R (or S) camphor vapors. The reason for this is that the dynamical effect of intermolecular collisions will be different. In order to explain this effect it is not sufficient to rely on theories of collision-induced line broadening[5] that leave out of consideration the statistical correlation between molecular rotation and translation. (This type of theory is exemplified by the well-known m and J diffusion models.[5]) The statistical correlation between $\mathbf{v}$, the center-of-mass translational molecular velocity and $\mathbf{J}$ the molecular angular momentum is identical for R and S camphor and exists at all vapor pressures. It vanishes

in the theoretical limit of infinite dilution, because in this limit, and in this limit only, the intermolecular potential energy vanishes. The correlation may be quantified with a moving frame matrix such as $C_{tr}(t) = \langle \mathbf{v}(t)\mathbf{J}^T(0) \rangle_m$, where $\langle\ \rangle_m$ denotes running time averaging with both $\mathbf{v}$ and $\mathbf{J}$ defined in this moving frame, for convenience that of the principal molecular moments of inertia. R and S enantiomers are physically different mirror images, and the cross-correlation matrix C_{tr} contains elements that are asymmetric in their time dependence.[24] The overall symmetry of C_{tr} for the R enantiomer is different from that of its S counterpart. The molecular dynamics for the R and S enantiomers are therefore different when looked at from the correct (and unique) viewpoint embodied in C_{tr}. If the R and S enantiomers are mixed in equal proportion, to give the racemic mixture, the asymmetric elements in C_{tr} cancel and vanish for all t, leaving other elements intact.[24] This is, essentially speaking, the effect of chiral discrimination in a dynamical context. The cross-correlation matrix C_{tr} behaves as it does because the R and S stereoisomers are mirror images, whose dynamical properties *in the laboratory frame* are all precisely identical to an observer who does not have the use of polarized radiation. A theory of molecular dynamics which does not consider C_{tr} is left with an impossible task—that of describing R and S identically and at the same time explaining why the laboratory-frame dynamical properties of mixtures of R and S are different because of chiral discrimination. It follows that these observable differences cannot be explained without considering C_{tr}. Therefore, these differences may be used to measure C_{tr} and cross-correlation functions like it. This must, and can only, be done by taking chiral discrimination fully into account in the Hamiltonian. Therefore the interpretation of spectral differences between RS and R or S is in principle a method of measuring those energy differences known as chiral discrimination.

Boiling point differences between RS and R or S liquids are known, and there are well-known density and refractive index differences at constant temperature. These are usually small, but sometimes there are differences of tens of degrees in the melting points of racemic mixture and enantiomer. Examples are the lactic acids, canadines, and 2-chlorobutanes, a relatively simple molecular structure where there is a 9-K difference[52] between the melting points of enantiomers and racemic mixture. In the solid state it is well known that these differences can be amplified greatly.[53,54] The spectral differences between RS and R or S in the molecular crystalline state are pronounced. In the infrared there are, for example, pronounced displacements in the frequency of fundamentals and lattice modes.[50,51] In the supercooled and glassy condition, various spectral properties of enantiomer and racemic mixtures are known which prove conclusively that there are large observable differences. Camphor provides a good example, with its well-

characterized "pseudo-eutectic" between rotator and λ phases at 1 bar below the normal melting points. Rossitter[54] has unearthed a spectacular difference in the Cole-Cole plot of *RS* and *R* or *S* camphor in the λ phase. The existence of Cole-Cole arcs for both enantiomers and racemic mixture implies the existence of a molecular dynamical process of some kind. Evans[53,55] has recently corroborated these findings to a limited extent in the far infrared in the room-temperature rotator phase, providing another spectral angle on the molecular dynamics. The far infrared results of Evans and radio-frequency data of Rossitter imply that the absorption of the *R* and *S* enantiomers is identical to unpolarized radiation but that the absorption of the racemic mixture (*RS* camphor) is distinctly different at essentially the same temperature. These results cannot be explained without recognizing the role of C_{tr} and taking chiral discrimination into account. In this context it is interesting that elements of C_{tr}, when properly normalized, increase in amplitude in the supercooled condition below the normal melting point for both chiral and achiral molecules.

Therefore, by looking at supercooled and glassy chiral molecules we maximize our chances of seeing laboratory-frame differences between an enantiomer and its racemic mixture. These differences cannot be explained in the theory of molecular diffusion without accounting for C_{tr}. The only theoretical method available for doing this in detail is computer simulation, and in this section we use this method to investigate the effect of chiral discrimination in the laboratory and moving frames of reference for some correlation functions of *sec*-butyl chloride supercooled in the amorphous condition to 50 K. This molecule is chosen for investigation because it is the simplest chiral system in which the difference between the melting points of enantiomers and racemic mixture is known to enough accuracy to verify that there is a large effect on the melting point of chiral discrimination.

Specifically in this section we investigate laboratory and moving-frame differences between the molecular dynamics of the *sec*-butyl chloride enantiomers and racemic mixture, both at equilibrium in the supercooled condition and in their response to an external electric field.

The details of the pair potential used in the simulations are given in Table I. This consists of an all-*trans* model of the *sec*-butyl chloride molecule with six moieties. The intermolecular pair potential is then built up with 36 site-site terms per molecular pair. Each site-site term is composed of two parts: Lennard-Jones and charge-charge. In this way, chiral discrimination is built in to the potential in a natural way. The phase-space average *R-R* (or *S-S*) potential is different from the equivalent in *R-S* interactions. The algorithm transforms this into dynamical time-correlation functions.

The effect of chiral discrimination at equilibrium is illustrated in Fig. 6 for the angular velocity acf of both enantiomers and racemic mixture at

TABLE I
Site-Site Potential for *trans-sec*-Butyl Chloride: Lennard-Jones and Partial Charge Terms

Moiety	$x(\mathbf{e}_3)$,[a] Å	$y(\mathbf{e}_1)$,[a] Å	(R) $z(\mathbf{e}_2)$,[a] Å	(S) $z(\mathbf{e}_2)$,[a] Å	ϵ/k, K	σ, Å	q, $\lvert e\rvert$
CH_3—	−2.14	−0.29	0.48	−0.48	158.6	4.0	0.04
CH_2—	−0.87	0.32	1.09	−1.09	158.6	4.0	0.028
Cl	0.40	0.00	−1.27	1.27	127.9	3.6	−0.177
C	0.40	−0.29	0.48	−0.48	35.8	3.4	0.001
H	0.40	−1.39	0.69	−0.69	10.0	2.8	0.068
CH_3—	1.67	0.32	1.09	−1.09	158.6	4.0	0.04

[a] Coordinates relative to center-of-mass, principal molecular moment-of-inertia frame.

50 K, in the supercooled liquid condition of the 2-chlorobutanes. There is little difference among the three cases, and this is buried in the statistical noise generated by the computer run. In the case of the center-of-mass velocity acf's in the same, equilibrium, condition (Fig. 7*a*) the difference between enantiomers and racemic mixture does, however, fall outside the noise, and this is an indication that the mixture of right and left stereoisomers has dynamical properties different from those of each component.

The effect of the strong external field is to accentuate this difference—using the method first developed for achiral molecules described earlier in this review—that of aligning the molecules in the "molecular dynamics" cube with an externally applied torque.[14-18] This may be used to simulate the effect of an electric field on an assembly of dipolar molecules using second-order

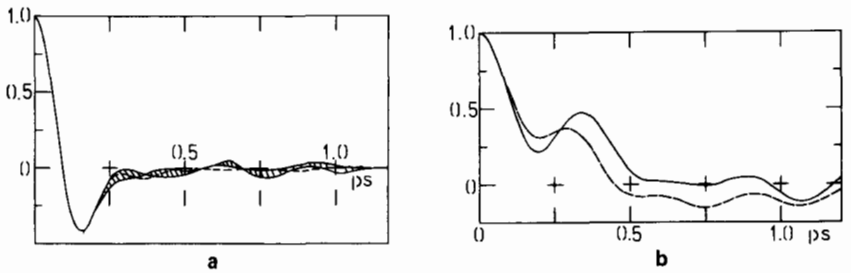

Figure 6. (*a*) 2-Chlorobutane at 50 K, 6×6 site–site potential, angular velocity autocorrelation functions. Crosshatching indicates computer noise difference between *R* and *S* enantiomers. (—) Racemic mixture. (*b*) As for (*a*), under the influence of a strong field **E**, producing a torque $-\mathbf{e}_3 \times \mathbf{E}$ in each molecule of the molecular dynamics sample. (1) (—) Racemic mixture; (2) (---) *R* enantiomer. Ordinate: Normalized correlation function; abscissa: time, ps.

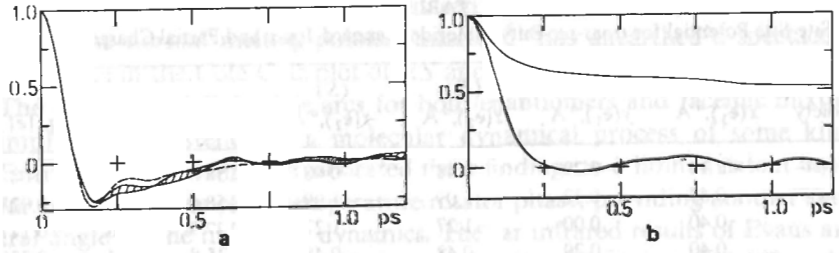

Figure 7. (*a*) As for fig. 6(*a*): center-of-mass linear velocity acf's (*b*) As for Fig. 6(*b*): racemic mixture. Ordinate: Normalized correlation function; abscissa: time, ps.

averages, or, a train of Gwatt electromagnetic pulses from a mode-locked laser. These methods have been described earlier, and here we concentrate only on the results of applying the torque to the $\mathbf{e}_3$ vector of the 2-chlorobutane molecules—enantiomers and racemic mixture.

The application of a powerful enough torque in this way reveals much about the hidden theoretical structure of the molecular liquid state, lending support to the reduced model theory of Grigolini.[5-7] For the supercooled 2-chlorobutanes we use an applied torque powerful enough to result in saturation of the component in the laboratory from $\langle e_{3z} \rangle = 1.0$. This is achieved quite easily because of the low temperature (50 K). Figure 6*b* shows that the effect on the angular velocity is pronounced, this function taking on a complex oscillatory form quite different from its counterpart at equilibrium (Fig. 6*a*). The decoupling effect of Grigolini is, however, small in this case because of the low temperature and high packing density of the supercooled environment. The envelope of the acf under the influence of the field is not much longer lived than that at equilibrium, although the structure of the acf is changed. The chiral discrimination effect seems to be enhanced by the external torque, that is, there is a greater difference between the acf's of enantiomer and racemic mixture. This should be checked, however, with more powerful computers and longer runs, to improve the statistics. Figure

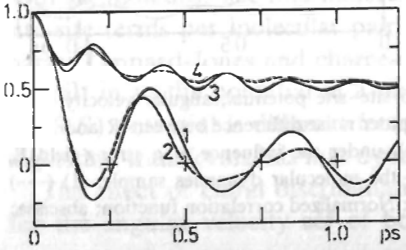

Figure 8. As for Fig. 6(*b*), angular momentum acf's. (1) Racemic mixture; (2) *R* enantiomer; (3) second moment,[5] racemic mixture; (4) second moment,[5] *R* enantiomer. Ordinate: Normalized correlation function; abscissa: time, ps.

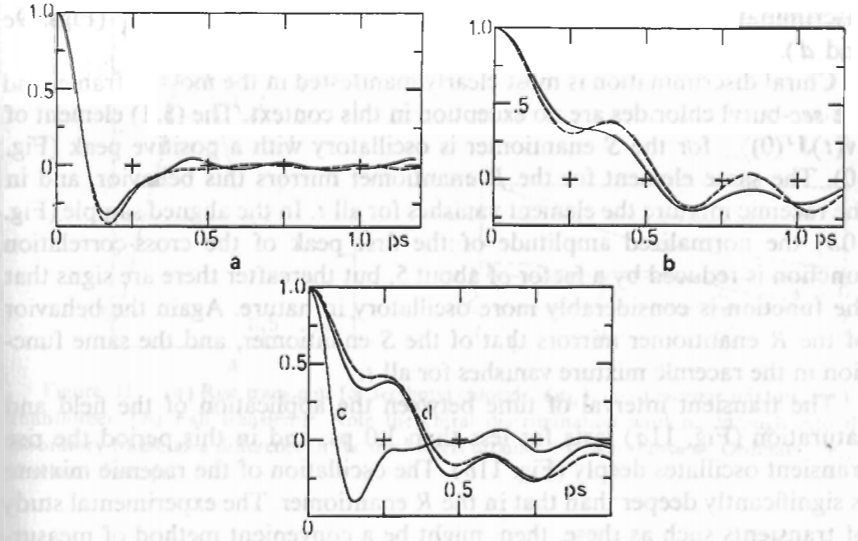

Figure 9. (*a*) As for Fig. 6(*a*), rotational velocity acf $\langle \dot{\mathbf{e}}_2(t) \cdot \dot{\mathbf{e}}_2(0) \rangle / \langle \dot{\mathbf{e}}_2^2 \rangle$. (—) *R* enantiomer, (---) racemic mixture. (*b*) As for Fig. 9*a*, aligned with an external field. (—) Enantiomer: (---) racemic mixture. Ordinate: Normalized correlation function; abscissa: time, ps. (*c*) *R* enantiomer $\langle \dot{\mathbf{e}}_1(t) \cdot \dot{\mathbf{e}}(0) \rangle / \langle \dot{e}_1^2 \rangle$ isotropic sample. (*d*) Aligned sample. (---) *R* enantiomer; (—) racemic mixture.

7*b* shows that the parallel effect on the center-of-mass velocity acf is much smaller, making the acf less oscillatory. It should be noted that the kinetic energy acf $\langle v^2(t) v^2(0) \rangle / \langle v^4 \rangle$ approaches a limit of 0.5 as $t \to \infty$. For an isotropic three-dimensional system the levels dictated[38] by Gaussian statistics is 0.6, that for a two-dimensional sample 0.5. This shows that the saturation by a field along the z axis has reduced the dimensionality of the molecular dynamics, one dimension being constrained by the field.

Some features of the Grigolini decoupling effect are shown more clearly in the angular momentum acf's (Fig. 8) for the aligned samples. These acf's are much different from their counterparts of Fig. 6, being more oscillatory and longer lived. The envelope of the oscillations measures the extent of the decoupling from the molecular thermal bath, as defined by Grigolini and coworkers. Again the effects of chiral discrimination seem to be visible clearly in the laboratory frame as a difference in period and amplitude of the acf oscillations for enantiomer and racemic mixture. The rotational velocity acf's exemplified in Fig. 9 are observable experimentally by far-infrared spectroscopy and also show the Grigolini decoupling effect in both enantiomer and racemic mixture (Figs. 9*a* and *b*). In this case also the effect of chiral

discrimination is clear, as in the rotational velocity acf's of $\dot{\mathbf{e}}_1$ (Figs. 9*c* and *d*).

Chiral discrimination is most clearly manifested in the moving frame, and the *sec*-butyl chlorides are no exception in this context. The (3,1) element of $\langle \mathbf{v}(t)\mathbf{J}^T(0)\rangle_m$ for the *S* enantiomer is oscillatory with a positive peak (Fig. 10). The same element for the *R* enantiomer mirrors this behavior, and in the racemic mixture the element vanishes for all *t*. In the aligned sample (Fig. 10*b*) the normalized amplitude of the first peak of the cross-correlation function is reduced by a factor of about 5, but thereafter there are signs that the function is considerably more oscillatory in nature. Again the behavior of the *R* enantiomer mirrors that of the *S* enantiomer, and the same function in the racemic mixture vanishes for all *t*.

The transient interval of time between the application of the field and saturation (Fig. 11*a*) lasts for less than 1.0 ps, and in this period the rise transient oscillates deeply (Fig. 11*b*). The oscillation of the racemic mixture is significantly deeper than that in the *R* enantiomer. The experimental study of transients such as these, then, might be a convenient method of measuring the dynamical effect of chiral discrimination in the liquid state. Deep transient oscillations such as these have been foreseen theoretically by Coffey and coworkers using the theory of Brownian motion.[3] The equivalent fall transients (Fig. 11*b*) are much longer lived than the rise transients and are not oscillatory. They decay more quickly than the equilibrium acf's. The effect of chiral discrimination in Fig. 11*b* is evident. Note that the system

$$\dot{\theta} = \omega$$

$$\dot{\omega} = -\gamma\omega - \frac{\mu E \sin\theta}{I} + f(t)$$

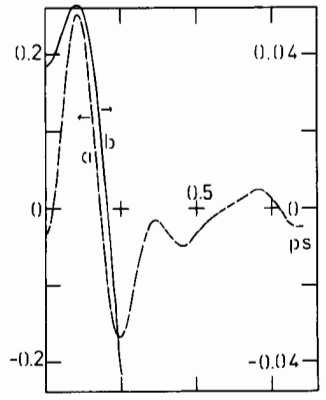

Figure 10. (*a*) (3,1) element of the cross-correlation function for the *R* enantiomer, $\langle \mathbf{v}(t)\mathbf{J}^T(0)\rangle$, $(\langle v_3(t)J_1(0)\rangle/(\langle v_3^2\rangle^{1/2}\langle J_1^2\rangle^{1/2}))$. (*b*) The same under the aligning field. Ordinate: Normalized cross-correlation function; abscissa, time, ps.

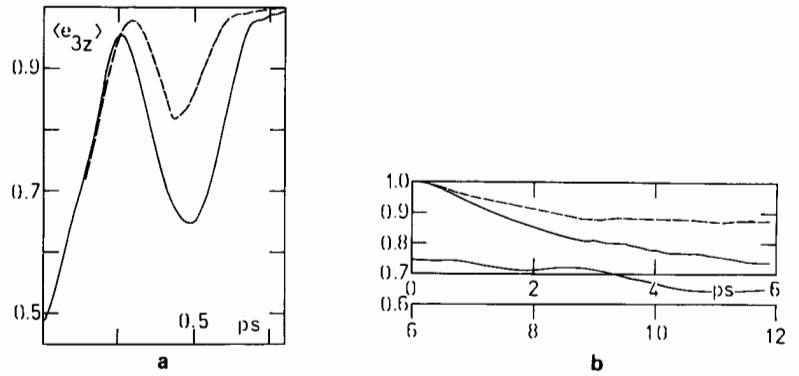

Figure 11. (*a*) Rise transients for *sec*-butyl chloride, $\langle e_{3z}\rangle$. (—) racemic mixture; (---) *R* enantiomer. (*b*) Fall transients: Note the chiral discrimination working through into the laboratory frame as a difference in the final levels attained by each transient. Ordinate: $\langle e_{3z}\rangle$; abscissa: time, ps.

as *E* becomes very large, results in the oscillating behavior of $\cos\theta$ as a trivial consequence of the fact that when $\omega_1 = (\mu E/I)^{1/2} \gg \gamma$ this is an inertial regime ($\cos\theta$ becomes non-Markovian as a consequence of the coupling $\mu E \sin\theta$). Finally, in Fig. 12 we illustrate the presence of rotation-translation coupling through the propeller effect. As the name implies, this is the translation of molecules induced by an applied torque. Baranova et al.[56] have suggested that this phenomenon could be used to separate *R* and *S* enantiomers physically from a racemic mixture by applying an alternating, circularly polarized, field. The simulations of Fig. 12 seem to imply that there is a very small net translational drift in the sample. The simple center-of-mass velocity components and $\langle v_x\rangle$, $\langle v_y\rangle$, and $\langle v_z\rangle$ gradually drift away from their initial zero values. The behavior of $\langle v_z\rangle$ in this respect for the racemic mixture and *R* enantiomer is different (Fig. 12*a*)—the components drift off in opposite directions. The equivalent drift in $\langle v_x\rangle$ is faster for the *R* enantiomer (Fig. 12*b*). The drift in $\langle v_y\rangle$ (Fig. 12*c*) is similar for the *R* enantiomer and the racemic mixture. Note that these results appear in the laboratory frame, so that a strong enough uniaxial electric field such as the one used in this paper seems to cause a *very small* amount of bulk movement of both the *R* enantiomer and racemic mixture, *but movement in different directions*. This is because the torque components applied externally in the simulation cause translation in different directions for the *R* and *S* enantiomers. The net translation in the racemic mixture is the resultant of these two vectors. Similar results are observable by computer simulation with circularly polarized fields. In conclusion, the application of an external torque seems to emphasize the role of rotation/translation and chiral discrimination in the

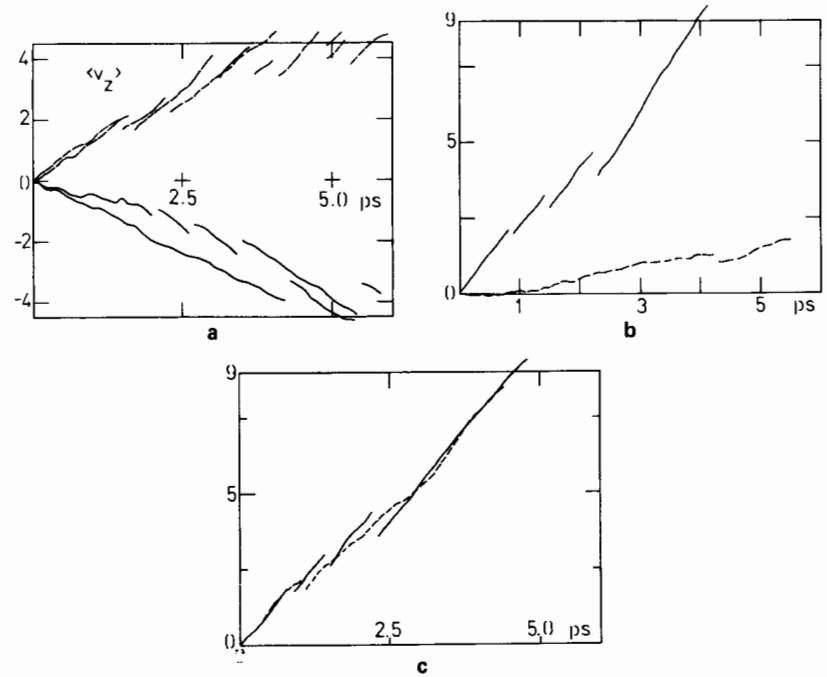

Figure 12. Velocity drift with applied field. (*a*) $\langle v_z \rangle$ (in program units; two runs); (---) *R* enantiomer; (—) racemic mixture. (*b*) $\langle v_x \rangle$; (—) *R* enantiomer; (---) racemic mixture. (*c*) $\langle v_y \rangle$; (—) *R* enantiomer; (---) racemic mixture. Abscissa time, ps.

condensed state dynamics of optically active molecules. *The results reported in this section are preliminary in nature* and should be supplemented by computations using better statistics for the calculation of equilibrium correlation functions and rise and fall transients.

A. Rise and Fall Transients in Fluorochloroacetonitrile

The real enantiomers of the fluorochloroacetonitrile molecule have been synthesized recently and are available for spectral investigation of their molecular dynamics. The first results on the simulation of liquid fluorochloroacetonitrile at 133 K, 1 bar, are reported in this section in the form of rise and fall transients for the enantiomers and racemic mixture. The site-site parameters for this simulation are given in Table II. The site symmetry in fluorochloroacetonitrile is such that the net dipole moment reverses in direction from *R* to *S* enantiomer. In the *R* and *S* enantiomers the transients are mirror images, and transient averages of the type[14-18] $\langle e_{2z}^{2n+1} \rangle$ vanish for all *n* in the racemic mixture. The effect of the field is therefore to produce a large *laboratory-frame* difference between the *R* and *S* enantiomers and mixtures.

TABLE II
Site-Site Potential for Fluorochloroacetonitrile: Lennard-Jones and Partial Charge Terms

Atom	$x(\mathbf{e}_3)$,[a] Å	$y(\mathbf{e}_1)$,[a] Å	(*R*) $z(\mathbf{e}_2)$,[a] Å	(*S*) $z(\mathbf{e}_2)$, Å	ϵ/k, K	σ, Å	$q/\lvert e \rvert$
N	0.75	−2.28	0.35	−0.35	47.8	3.0	−0.16
C_1	0.27	−1.29	−0.03	0.03	35.8	3.4	−0.02
C_2	−0.34	−0.05	−0.51	0.51	35.8	3.4	0.03
H	−0.34	−0.38	−1.59	1.59	10.0	2.8	0.51
Cl	0.61	1.33	0.07	−0.07	127.9	3.6	−0.16
F	−1.64	0.06	0.02	−0.02	54.9	2.7	−0.20

[a]Atomic coordinates w.r.t center of mass, principal molecular moment-of-inertia frame.

Therefore, the external electric field can be used to identify the differences between the molecular dynamics of enantiomers and their mixtures. The rise transients from the simulation show a strong field dependence, becoming much more rapid as the field strength increases.[2] The *R* and *S* enantiomers mirror each other in their field dependence for a averages of the form $\langle e_{2z}^{2n+1} \rangle$ and are identical for even averages of the type $\langle e_{2z}^{2n} \rangle$. *The fall transients decay much more rapidly than the equivalent autocorrelation functions at equilibrium*. The effect is pronounced for saturating field strengths (i.e., $\langle e_{2z} \rangle \doteq \pm 1.0$). As the external field strength decreases, the fall transients approach the equilibrium autocorrelation function. The deexcitation effect is clearly, therefore, a function of the external field first applied to the sample and then removed, that is, the fall transient behavior from the computer simulation depends on the history of the field application.

1. *Rototranslational Correlations in the Laboratory Frame of Reference*

To end this section and the review, we mention briefly the first results from the simulation on *laboratory-frame cross-correlation* of the type $\langle \mathbf{v}(t)\mathbf{J}^T(0) \rangle$. Here **v** is the molecular center-of-mass linear velocity and **J** is the molecular angular momentum in the usual laboratory frame of reference. For chiral molecules the center-of-mass linear velocity **v** seems to be correlated *directly* in the laboratory frame with the molecule's own angular momentum **J** at different points *t* in the time evolution of the molecular ensemble. This is true in both the presence and absence of an external electric field. *These results illustrate the first direct observation of elements of* $\langle \mathbf{v}(t)\mathbf{J}^T(0) \rangle$ *in the laboratory frame of reference*. The racemic modification of physical and molecular dynamical properties depends, therefore, on the theorem $\langle \mathbf{v}(t)\mathbf{J}^T(0) \rangle \neq 0$ in both static and moving frames of reference. An external electric field enhances considerably the magnitude of the cross-correlations.

Acknowledgments

The SERC and University of Wales are thanked for generous financial support.

References

1. H. Benoit, *Ann. Phys.*, **6**, 561 (1951).
2. A. Morita and H. Watanabe, *J. Chem. Phys.*, **70**, 4708 (1979).
3. W. T. Coffey, C. Rybarsch, and W. Schroer, *Chem. Phys. Lett.*, **99**, 31 (1983).
4. W. T. Coffey and B. V. Paranjape, *Proc. Roy. Irish Acad.*, **78A**, 17 (1978).
5. M. W. Evans, G. J. Evans, W. T. Coffey and P. Grigolini, *Molecular Dynamics*, Wiley-Interscience, New York, 1982, Chapters 9 and 10.
6. W. T. Coffey, M. W. Evans, and P. Grigolini, *Molecular Diffusion and Spectra*, Wiley-Interscience, New York, 1984, Chapters 7–9.
7. P. Grigolini, *Nuovo Cimento*, **63B**, 174 (1981).
8. D. Fincham and D. Heyes, (Vol. 63 of this series).
9. P. Grigolini, *Mol. Phys.*, **31**, 1717 (1976).
10. P. Grigolini and A. Lami, *Chem. Phys.*, **30**, 61 (1978).
11. P. Grigolini, *Chem. Phys. Lett.*, **47**, 483 (1977).
12. P. Grigolini, *Chem. Phys.*, **38**, 389 (1979).
13. See ref. 5, Chapter 9.
14. M. W. Evans, *J. Chem. Phys.*, **76**, 5473 (1982).
15. M. W. Evans, *J. Chem. Phys.*, **76**, 5480 (1982).
16. M. W. Evans, *J. Chem. Phys.*, **77**, 4632 (1982).
17. M. W. Evans, *J. Chem. Phys.*, **78**, 925 (1983).
18. M. W. Evans, *J. Chem. Phys.*, **78**, 5403 (1983).
19. B. Bagchi and D. W. Oxtoby, *J. Phys. Chem.*, **86**, 2197 (1982).
20. B. Bagchi and D. W. Oxtoby, *J. Chem. Phys.*, **77**, 1391 (1982).
21. M. W. Evans, P. Grigolini, and F. Marchesoni, *Chem. Phys. Lett.*, **95**, 544 (1983).
22. M. W. Evans, P. Grigolini, and F. Marchesoni, *Chem. Phys. Lett.*, **95**, 548 (1983).
23. E. Praestgaard and N. G. van Kampen, *Mol. Phys.*, **43**, 33 (1981).
24. M. W. Evans, *Phys. Rev. Lett.*, **50**, 371 (1983).
25. M. Ferrario, M. W. Evans, and W. T. Coffey, *Adv. Mol. Rel. Int. Proc.*, **23**, 143 (1982).
26. C. J. Reid, *Mol. Phys.*, **49**, 331 (1983).
27. C. Brot, G. Bossis, and P. Hesse-Bezot, *Mol. Phys.*, **40**, 1053 (1980).
28. L. Onsager, *J. Amer. Chem. Soc.*, **58**, 1486 (1936).
29. See ref. 6, appendix to Chapter 5.
30. M. Andretta et al., (Vol. 63 of this series).
31. C. J. Reid, Ph.D. thesis, University of Wales, presented in brief as Chapter 4 of ref. 5.
32. J. T. Lewis, J. R. McConnell, and B. K. P. Scaife, *Proc. Roy. Irish Acad.*, **76A**, 43 (1976).
33. J. H. Calderwood and W. T. Coffey, *Proc. Roy. Soc., A*, **356**, 269 (1977).
34. M. W. Evans, *Phys. Rev. A*, **30(4)**, 2062 (1984).
35. M. W. Evans, *Chem. Phys. Lett.*, **50**, 371 (1983).

36. W. T. Coffey, *Mol. Phys.*, **38**, 437 (1979).
37. S. Kielich, in *Dielectric and Related Molecular Processes*, Vol. 1, M. Davies, ed., The Chemical Society, London, 1972.
38. B. J. Berne and R. Pecora, *Dynamic Light Scattering with Reference to Physics, Chemistry and Biology*, Wiley-Interscience, New York, 1976.
39. J. P. Ryckaert, A. Bellemans, and G. Ciccotti, *Mol. Phys.*, **44**, 979 (1981).
40. R. J Abbott and D. W. Oxtoby, *J. Chem. Phys.*, **72**, 3972 (1980).
41. R. Kubo, *Adv. Chem. Phys.*, **15**, 101 (1969).
42. P. Grigolini, *J. Chem. Phys.*, **74**, 1517 (1981).
43. M. Ferrario and P. Grigolini, *J. Chem. Phys.*, **74**, 235 (1981).
44. R. Zwanzig, *Lecture Notes in Physics*, **132**, 198 (1980).
45. P. Grigolini, *J. Stat. Phys.*, **27**, 283 (1982).
46. B. J. Berne and G. D. Harp, *Adv. Chem. Phys.*, **17**, 143 (1968).
47. U. Balucani, R. Vallauri, V. Tognetti, P. Grigolini, and P. Marin, *Z. Phys.*, **B49**, 181 (1982).
48. S. Faetti, P. Grigolini, and F. Marchesoni, *Z. Phys.*, **B47**, 353 (1982).
49. A. Balucani, V. Tognetti, R. Vallauri, P. Grigolini, and M. P. Lombardo, *Phys. Lett.*, **86A**, 426 (1981).
50. S. F. Mason, *Molecular Optical Activity and Chiral Discriminations*, C.U.P., Cambridge, (1982).
51. J. Jacques, A. Collet, and S. H. Wilen, *Enantiomers, Racemates and Resolutions*, Wiley, New York, 1981.
52. J. Timmermans and F. Martin, *J. Chim. Phys.*, **25**, 411 (1928).
53. G. J. Evans, *J. Chem. Soc., Faraday Trans II*, in press.
54. V. Rossitter, *J. Phys.* **D5**, 1969 (1972).
55. M. W. Evans, *J. Chem. Soc., Faraday Trans II*, **79**, 719 (1983).
56. N. B. Baranova and B. Y. Zeldovich, *Chem. Phys. Lett.*, **57**, 435 (1978).